Title Page

Epstein–Barr virus exploits host endocytic machinery for cell-to-cell viral transmission rather than a virological synapse

Short title; Role of endocytic pathway in cell-to-cell EBV transmission

Asuka Nanbo[1]*, Kunihiro Kachi[2], Hironori Yoshiyama[3], and Yusuke Ohba[1]

Department of Cell Physiology, Hokkaido University Graduate School of Medicine, N15 W7, Kita-ku, Sapporo, Japan[1], Graduate School of Pharmaceutical Sciences, Hokkaido University, N12 W6, Kita-ku, Sapporo, Japan[2], Department of Microbiology, Shimane University Faculty of Medicine, 89-1, Enya-cho, Izumo, Shimane, Japan[3]

*Corresponding author.

Mailing address: Department of Cell Physiology, Hokkaido University Graduate School of Medicine, N15 W7, Kita-ku, Sapporo 060-8638, Japan.

Phone: +81(11) 706-5158

Fax: +81(11) 706-7877

Email: nanboa@med.hokudai.ac.jp

The word counts for the abstract: **250**; the text: **5770**

Abstract

Epstein–Barr virus (EBV) establishes a life-long latent infection in B lymphocytes and often is found in epithelial cells. Several lines of evidence indicate that viral transmission mediated by cell-to-cell contact is the dominant mode of infection by EBV for epithelial cells. However, its detailed molecular mechanism has not been fully elucidated. We investigated the role of host membrane trafficking machinery in this process. We have found that adhesion molecules critical for this process are expressed in EBV-positive, -negative Burkitt's lymphoma (BL) cells and multiple epithelial cell lines. Treatment with blocking antibodies against β1 and β2 integrin families and their ligands suppressed EBV transmission in a dose-dependent manner. We also confirmed that adhesion molecules are up-regulated in co-cultured BL cells. Immunofluorescence staining revealed that the intracellular adhesion molecule 1 (ICAM-1) distributed to the cell surface and partially co-localized with recycling endosomes in co-cultured BL cells. Moreover, cell-to-cell EBV transmission was inhibited upon blocking endocytic recycling by expression of a dominant-negative form of a small GTPase Rab11 or by knockdown of Rab11, supporting the notion that the endocytic pathway-dependent trafficking of ICAM-1 to the cell surface of BL cells contributes to viral transmission by stabilizing cell-to-cell contact between the donor cells and recipient cells. Finally, we demonstrated that co-cultivation up-regulated clathrin-mediated endocytosis in the recipient cells, allowing EBV to be internalized. Taken together, our findings demonstrate that EBV exploits host endocytic machinery in both donor and recipient cells, a process which is facilitated by cell-to-cell contact, thereby promoting successful viral transmission.

Keywords

Epstein-Barr virus; cell-to-cell viral transmission; adhesion molecule; recycling endosome; endocytosis

Introduction

Epstein–Barr virus (EBV), a human gamma herpesvirus, establishes a persistent latent infection in B lymphocytes and often is found in epithelial cells. EBV also causes lymphomas and epithelial malignancies such as Burkitt's lymphoma (BL), Hodgkin's disease, nasopharyngeal carcinoma, and gastric cancer (Kieff & Rickinson, 2001).

The mechanism by which EBV infects B lymphocytes has been well characterized. EBV attaches to B lymphocytes through a direct interaction of the EBV major outer envelope glycoprotein complex gp350/220 with the complement receptor CD21 (Fingeroth *et al.*, 1999; Nemerow *et al.*, 1987; Tanner *et al.*, 1987; Tanner *et al.*, 1988), leading to endocytosis-mediated internalization of EBV. Fusion of the viral envelope with the endosomal membrane of B cells is triggered by the interaction of a second envelope glycoprotein, gp42, with HLA class II (Iizasa *et al.*, 2012; Li *et al.*, 1997; Nemerow *et al.*, 1987; Oda *et al.*, 2000). In contrast, the mechanism by which EBV infects epithelial cells remains less well defined. Infection of cell-free EBV into epithelial cells appears to be mediated by fusion of the viral envelope with the cellular plasma membrane. Human epithelial cells are CD21-negative or some epithelial cells in culture express CD21 at low levels, resulting in a high resistance to cell-free EBV infection (Fingeroth *et al.*, 1999; Imai *et al.*, 1998). Several lines of evidence indicate that cell-to-cell viral transmission is a dominant mode for infection of EBV into epithelial cells. The efficiency of EBV infection in epithelial cells is significantly enhanced by co-culturing them with EBV-positive B cells relative to cell-free infection (Chang *et al.*, 1999; Imai *et al.*, 1998; Nanbo *et al.*, 2012; Speck & Longnecker, 2000). These studies support a model in which EBV-infected B cells that migrate into the epithelial stroma or intraepithelial

space contribute to efficient EBV transmission into epithelial cells *via* cell-to-cell contact. However, the detailed molecular mechanisms of cell-to-cell EBV transmission remain to be fully elucidated.

It has been shown that cell-to-cell infection of retroviruses such as human T-cell lymphotropic virus (HTLV) and human immunodeficiency virus (HIV)-1 is mediated by the virological synapse (VS). The VS is an actin- and microtubule-dependent stable adhesive junction across which retroviruses can be efficiently transferred from virus-infected dendritic cells or T cells to non-infected target T cells without cell-cell fusion (Agosto *et al.*, 2015; Jolly & Sattentau, 2004). In the process of the VS formation, cell organelles such as the microtubule organizing center (MTOC) and endosomes are reoriented toward the interface of contacted cells, resulting in active recruitment of viral antigens, cellular receptors, and adhesion molecules toward the site of conjugation (Jolly & Sattentau, 2004; Zhong *et al.*, 2013). Assembly and budding of retroviruses is targeted to the VS, leading to subsequent fusion of the viral envelop with the plasma membrane or with the endosome of recipient cells (Bosch *et al.*, 2008; Dale *et al.*, 2011; Puigdomenech *et al.*, 2009).

Previously we established an assay to assess the efficiency of viral transmission mediated by cell-to-cell contact by co-culturing latently EBV-infected cells and EBV-negative epithelial cells. By use of this assay, we demonstrated that cell-to-cell contact induces multiple cell signaling pathways in BL cells and epithelial cells, contributing to the induction of the viral lytic cycle in BL cells and the enhancement of viral transmission to epithelial cells (Nanbo *et al.*, 2012).

In the present study, we have assessed the role of the host membrane trafficking machinery in cell-to-cell EBV transmission. We observed that critical adhesion molecules are up-regulated in EBV-positive and -negative BL cells when co-cultured with epithelial cells. In particular, co-cultivation induced the trafficking of ICAM-1 to the cell surface in BL cells in a vesicle recycling-dependent manner. We also observed that direct cell-to-cell contact enhanced clathrin-dependent endocytosis in recipient cells, which supported progeny EBV virions entering the recipient cells. There were no significant differences between EBV-positive and -negative BL cells in the expression levels of adhesion molecules in co-cultured cells, the efficiency of cell-cell contact-mediated up-regulation of adhesion molecules, the recycling, endosome-dependent translocation of ICAM-1, and the up-regulation of endocytosis. Taken together, our observations show that EBV exploits pre-existing host endocytic machinery for its establishment of efficient viral transmission, a mechanism distinct from that of the VS employed by HIV.

Results

Identifying adhesion molecules expressed on Akata cells and epithelial cells.

Previously we established an assay to assess the efficiency of cell-to-cell transmission of EBV by co-culturing EBV-positive BL cells with EBV-negative epithelial cells (Nanbo *et al.*, 2012). We used the BL-derived Akata$^-$ EBV-eGFP cells, which are latently infected with a recombinant Akata-derived strain of EBV encoding eGFP (Maruo *et al.*, 2001a), with the EBV-negative human gastric epithelial cell lines (AGS and NU-GC-3 cells) and African green monkey kidney epithelial cell line (Vero-

E6 cells). The transmission of EBV-eGFP into the epithelial cells was analyzed by quantifying the percentage of eGFP-positive cells with flow cytometry.

The role of adhesion molecules, such as ICAM-1 and LFA-1 in the VS-mediated retrovirus infection has been characterized and found to be critical (Jolly & Sattentau, 2004; Zhong *et al.*, 2013).

In the present study, we investigated the role of adhesion molecules in cell-to-cell transmission of EBV. First we assessed the expression of CD11a (or αL subunit), and CD18 (or β2 subunit), which are components of αLβ2 integrin (or leukocyte function associated antigen; LFA-1) and known to participate in VS-mediated viral transmission, in EBV-positive Akata (Akata^{+}), -negative Akata (Akata^{-}), Vero-E6 cells, AGS cells, and human nasopharyngeal carcinoma CNE1 cells by flow cytometry. We also examined the expression of CD49d (or α4 integrin subunit), CD49e (or α5 subunit) and CD29 (or β1 subunit), which are components of α4β1 (or very late antigen 4; VLA4) and α5β1 integrins (or VLA5) in these cell lines. Moreover, the expression of VCAM-1 and fibronectin, which are ligands for β1 integrin and ICAM-1, which is a ligand of β2 integrin were analyzed. We also assessed the expression of αvβ5 and αvβ6, two molecules which have been shown to interact with gHgL and lead to the fusion of viral envelope and the plasma membrane of epithelial cells (Chesnokova & Hutt-Fletcher, 2011). Akata^{+} (Fig. 1a), Akata^{-} (Fig. 1b), Vero-E6 (Fig. 1c), AGS (Fig. 1d) and CNE1 (Fig. 1e) cells expressed all of these adhesion molecules. Although the expression levels of individual adhesion molecules varied among the examined cell lines, no significant differences were observed between EBV-positive and -negative BL cells.

Blocking antibodies to adhesion molecules inhibit cell-to-cell transmission of EBV

We examined the role of these adhesion molecules and their ligands in cell-to-cell transmission of EBV with blocking antibodies. Akata$^-$ EBV-eGFP cells and individual epithelial cells were pre-treated with blocking antibodies against CD49d, CD49e, CD29, VCAM-1, ICAM-1, αvβ6, or αvβ6 followed by co-cultivation in the presence of each of these antibodies. To enhance our detection of viral transmission, we cross-linked the cell surface IgG of Akata$^-$EBV-eGFP by adding F(ab')2 fragments of goat antihuman IgG polyclonal antibody (αhIgG) to induce the viral lytic cycle (Takada, 1984; Takada *et al.*, 1991; Takada & Ono, 1989). Consistent with our previous report (Nanbo *et al.*, 2012), co-culturing with Akata$^-$EBV-eGFP led to approximately 5% of the cell population being infected. αIgG-treatment increased the detected transmission efficiency up to approximately 11% in Vero-E6 cells (Fig. 2a). Approximately 5% and 7% of the cell population was infected by EBV-eGFP in the presence of αIgG in AGS and CNE1 cells, respectively (Fig. 2a).

All antibodies against β1 and β2 integrins and their ligands suppressed EBV transmission to Vero-E6 (Fig. 2b), AGS and CNE1 (Fig. 2c) cells in a dose-dependent manner. In contrast, treatment with the antibodies against αvβ5, αvβ6 and estrogen receptor (ER), which are also expressed in both Akata cells and epithelial cells (Fig.1), exhibited no effect on viral transmission (Fig. 2b and 2c), suggesting that cell-to-cell transmission of EBV was specifically dependent on cell contact through an interaction between β1 and β2 integrins and their ligands. Moreover our findings also indicate that CD49e, VCAM-1, and fibronectin, which are not known to participate in VS-mediated retrovirus infection do contribute to the cell-to-cell transmission of EBV.

Cell-to-cell contact up-regulates expression of adhesion molecules in co-cultured BL cells.

We assessed whether direct cell-to-cell contact modulates the expression of β1 and β2 integrins and their ligands in co-cultured cells to determine if co-cultivation facilitates viral transmission beyond the juxtaposing of cells. Akata$^+$ or Akata$^-$ cells were co-cultured with Vero-E6 cells for 6 h and harvested separately. To insure the harvested cells did not contain co-cultured donor cells, the expression of human leukocyte antigen (HLA)-DR or caveolin-1 (Cav1) in the harvested cells was analyzed by flow cytometry. HLA-DR is the class II histocompatibility molecule constitutively expressed on antigen-presenting cells including B cells, and T lymphocytes only after activation (Trowsdale *et al.*, 1991). Cav1 is an epithelial cell marker (Couet *et al.*, 2001). Both Akata$^+$ and Akata$^-$ cells expressed HLA-DR similarly and its expression was up-regulated after a 6 h-long co-cultivation (Fig. 3a and 3c). The expression of HLA-DR in Vero-E6 was low compared with that in BL cells and its expression did not change significantly (Fig. 3a and 3c). Cav1 was expressed in Vero-E6 cells similarly in the presence and absence of cell contact (Fig. 3b and 3d). EBV-positive and -negative Akata cells were almost Cav1-negative and its expression did not change by cell contact (Fig. 3b and 3d). The data indicate that the BL cells and Vero-E6 cells were successfully harvested separately. CD29, VCAM-1, and ICAM-1 were found to be up-regulated in both Akata$^+$ and Akata$^-$ cells after a 6 h-long co-cultivation (Fig. 3e and 3g). These BL cells expressed proteins at different levels: CD49d and ICAM-1 were higher in Akata$^+$, and CD11a and fibronectin were higher in Akata$^-$ (Fig. 3e and 3g). In contrast, the recipient Vero-E6 cells did not

change their levels of individual adhesion molecules when co-cultivated with either the EBV-positive and -negative BL cells (Fig. 3f and 3h). These measurements show that critical adhesion molecules are up-regulated in BL cells on their contact with epithelial cells.

Cell-to-cell contact promotes the translocation of ICAM-1 to the plasma membrane of co-cultured BL cells.

Because critical adhesion molecules were up-regulated in co-cultured EBV-positive and -negative BL cells (Fig. 3e and 3g), we examined the kinetics of expression of ICAM-1 to determine if its increased expression could contribute to transmission of EBV. ICAM-1 was up-regulated in both EBV-positive and -negative Akata cells after only 1 h-long of co-cultivation and its up-regulated status was maintained for 24 h (Fig. 4a and 4c). In contrast, the expression of ICAM-1 did not change and even slightly down-regulated in co-cultured Vero-E6 cells (Fig. 4b and 4d). We also examined the subcellular distribution of ICAM-1 in co-cultured cells by immunofluorescent staining. In the absence of cell-to-cell contact, ICAM-1 was distributed in the plasma membrane and cytoplasm as punctate signals in EBV-positive and -negative Akata cells (Fig. 4e and 4f). ICAM-1 moved to the plasma membrane after a 2 h-long co-cultivation, and the distribution persisted up to 24 h positioning it specifically and temporally to participate in EBV's transmission. In contrast, ICAM-1 was predominantly distributed diffusely in the cytoplasm in Vero-E6 cells and its distribution did not change under co-cultivation (Fig. 4g and 4h).

Some ICAM-1 localized to recycling endosomes in co-cultured BL cells.

We investigated the mechanism by which ICAM-1 distributed to the plasma membrane in co-cultured BL cells (Fig. 4e and 4f). Previous studies have demonstrated that endocytic recycling contributes to the transport of various adhesion molecules to the plasma membrane (Desclozeaux *et al.*, 2008; Diestel *et al.*, 2007; Lock & Stow, 2005; Mamdouh *et al.*, 2003). To determine whether this pathway is also involved in the cell-to-cell contact-induced translocation of ICAM-1, we investigated the subcellular localization of Rab11, a small GTPase in co-cultured Akata cells by immunofluorescent staining. Rab11 associates with recycling endosomes and regulates exocytosis and recycling processes to transport proteins to the cell surface (Kelly *et al.*, 2012; Ren *et al.*, 1998; Welz *et al.*, 2014). Rab11 also localizes to the trans-Golgi network (TGN) and post-Golgi vesicles, and has been implicated in the trafficking between the TGN and the endosomal recycling compartments through the regulated secretion pathway (Gromov *et al.*, 1998). In the absence of co-cultivation, ICAM-1 (green) distributed in the cytoplasm and plasma membrane as punctate signals in EBV-positive and -negative Akata cells (Fig. 5a and b, top, left). Rab11 (red) predominantly distributed in the perinuclear regions and some fraction of the protein distributed in the cytoplasm and the plasma membrane (Fig. 5a and b, top, middle), which did not co-localize with ICAM-1. In contrast, in co-cultured EBV-positive and -negative Akata cells, ICAM-1 distributed to the periphery of the cells and its cytoplasmic fraction partially co-localized with Rab11 (Fig. 5a and 5b, bottom), consistent with ICAM-1's being translocated to the plasma membrane *via* Rab11-dependent recycling. We also visualized the distribution of ICAM-1 and Rab11 in the series of Z-stacks in co-cultured Akata^{+} cells. ICAM-1 diffusely distributed to the

peripheral region of the plasma membrane (Fig. 5c), which was distinct from the tight distribution of adhesion molecules that is observed in the VS.

Rab11-dependent recycling endocytic pathway contributes to the EBV transmission mediated by cell-to-cell contact.

Because ICAM-1 partially co-localized with Rab11 in the cytoplasm of co-cultured BL cells (Fig. 5), we investigated the role of Rab11 in cell-to-cell contact-mediated EBV transmission. We transiently expressed a dominant-negative form of Rab11 that has an amino acid substitution (N25S) (Chen *et al.*, 1998) in Akata$^-$ EBV-eGFP cells (Fig. 6a) and assessed its effect on both the distribution of ICAM-1 in donor cells and on EBV transmission. Expression of Rab11 N25S in Akata$^-$ EBV-eGFP cells suppressed translocation of ICAM-1 to the plasma membrane of donor cells (Fig. 6b and c) and viral transmission (Fig. 6d). We also knocked down Rab11a and Rab11b isoforms in Akata$^-$ EBV-eGFP cells with a small interference RNA (siRNA). Rab11a and Rab11b share 90% amino acid sequence identity. Rab11a is expressed ubiquitously, predominantly localizes to recycling endosomes, and functions in the recycling of a wide range of molecules to the cell surface (Gromov *et al.*, 1998). Rab11b is expressed in the heart, brain and testes and functions in recycling of molecules in polarized cells (Silvis *et al.*, 2009). EBV transmission was partially inhibited by a single knock-down of Rab11 isoforms, and synergistically inhibited by knock-down of both isoforms (Fig. 6e and 6f). These results taken together indicate that cell-to-cell EBV transmission occurred in a Rab11-dependent manner, likely mediated by translocation of ICAM-1 to the cell surface.

Cell-to-cell contact facilitates clathrin-dependent endocytosis in the recipient cells, which contribute to infection of EBV

Previously we demonstrated that cell contact induces the viral lytic cycle in the donor cells (Nanbo *et al.*, 2012), however, little is known about the mechanism by which newly generated EBV virions enter Vero-E6 cells. To illuminate the mechanism that is involved in this process, we assessed the role of endocytosis in EBV transmission. We performed EBV transmission assays in the presence of dynasore (Newton *et al.*, 2006), which is a specific inhibitor for dynamin, a large GTPase that plays an essential role in vesicle scission during clathrin- and caveolae-dependent endocytosis (Orth *et al.*, 2002). Treatment with dynasore suppressed EBV transmission in a dose-dependent manner (Fig. 7a). We also transiently expressed a wild-type dynamin 2 (wtDyn2) and a dominant-negative form of dynamin 2 that has an amino acid substitution (Dyn2 K44A) (Orth *et al.*, 2002) in Vero-E6 cells (Fig. 7b), and assessed their effect on EBV transmission. The expression of wtDyn2 up-regulated viral transmission (Fig. 7c). In contrast, the expression of Dyn2 K44A suppressed viral transmission (Fig. 7c). These results indicate that EBV was transmitted to Vero-E6 cells through dynamin-dependent endocytosis. Treatment with NH_4Cl, which blocks acidification of endosomes, also interfered with viral transmission (Fig. 7d), indicating that EBV virions subsequently fuse in endosomal compartments in a low-pH-dependent manner. Previously we demonstrated that the lytic cycle is induced in Akata$^+$ cells by co-cultivation with Vero-E6 cells. To exclude the possibility that the inhibitors inhibited EBV replication in co-cultured B cells, we analyzed the effect of these inhibitors on the expression of the viral lytic gene, gp350 (Maruo *et al.*, 2001b; Nemerow *et al.*, 1987) by flow cytometric analysis. The expression

of gp350 was enhanced under the treatment of αhIgG (Fig. 7e). Treatment of 1 μM Dynasore or 20 mM NH_4Cl did not impair αhIgG-induced gp350 expression (Fig. 7e), indicating that these inhibitors specifically block the endocytosis-mediated internalization process in recipient cells.

To identify the endocytic pathway for EBV transmission, we examined the effect of inhibiting the clathrin-heavy chain (CHC), Cav1, or sorting nexin 1 (SNX1) in Vero-E6 cells with siRNA. CHC, Cav1, and SNX1 play roles in clathrin-, caveolae-, and macropinocytosis-mediated internalization, respectively (Kerr *et al.*, 2006; Manninen *et al.*, 2005; Moskowitz *et al.*, 2005). Down-regulation of CHC expression significantly suppressed EBV transmission (Fig. 8a and 8b), indicating that clathrin-mediated endocytosis likely contributes to EBV transmission. However, viral transmission was not blocked by down-regulation of Cav1 and SNX1 (Fig. 8b), further supporting the conclusion that caveolae-mediated endocytosis and macropinocytosis were not important for EBV transmission. Finally we examined whether direct cell contact enhances clathrin-mediated endocytosis in Vero-E6 cells. $Akata^+$ and $Akata^-$ cells were co-cultured with Vero-E6 cells for 6 h in the presence of fluorescently labeled transferrin, a specific ligand of the clathrin-mediated pathway. Uptake of transferrin was enhanced in Vero-E6 cells that were co-cultured with EBV-positive and -negative Akata cells (Fig. 8d). Furthermore its uptake was suppressed by down-regulation of CHC in Vero-E6 cells (Fig. 8c and 8d). The data indicates that cell-cell contact up-regulates clathrin-mediated endocytosis in recipient cells, leading to internalization of progeny EBV replicated in donor cells.

Discussion

Here, we show that EBV exploits host endocytic machinery to establish successful cell-to-cell transmission into epithelial cells. By use of a co-cultivation system with BL cells and various epithelial cells, we demonstrated that (i) a variety of adhesion molecules are expressed in EBV-positive, -negative Akata cells, and multiple epithelial cells (Fig. 1); and the interaction between β1 and β2 integrins, and their ligands contribute to viral transmission (Fig. 2); (ii) multiple adhesion molecules are up-regulated in co-cultured BL cells (Fig. 3); (iii) ICAM-1 distributes to the plasma membrane in co-cultured BL cells (Fig. 4) in a recycling endosome-dependent manner (Fig. 5 and 6); and transmission of EBV virions into epithelial cells is mediated by clathrin-dependent endocytosis, which is accelerated by co-cultivation (Fig. 7 and 8).

In the VS-mediated retrovirus transmission, the interaction between LFA-1 (αLβ2) in the recipient $CD4^+$ T cells and ICAM-1 in virally infected dendritic cells (Gilbert *et al.*, 2007; Groot *et al.*, 2006; Gummuluru *et al.*, 2002; Wang *et al.*, 2009) and T cells (Hioe *et al.*, 2001; Jolly *et al.*, 2004; Jolly *et al.*, 2007; Tardif & Tremblay, 2003; 2005) is important for viral transmission. In contrast, little is known about the role of β1 integrin in the VS. Our data indicate that both β1 and β2 integrins and their ligands are expressed in BL cells and epithelial cells (Fig. 1) and that their interaction contributes to EBV transmission (Fig. 2), suggesting that a bidirectional interaction of multiple adhesion molecules leads to efficient EBV transmission. We observed that individual blocking antibodies for various adhesion molecules suppressed viral transmission moderately (Fig. 2), suggesting that multiple adhesion molecules may contribute to it in a complementary fashion.

We observed that direct cell contact up-regulated several adhesion molecules in BL cells (Fig. 3e and 3g). In particular, ICAM-1 rapidly distributed to the plasma membrane of Akata cells even within a 1 h-long co-cultivation (Fig. 4a, 4c, 4e and 4f), which is unlikely to be mediated by *de novo* synthesis of ICAM-1. Moreover, a fraction of ICAM-1 partially co-localized with Rab11 in the cytoplasm (Fig. 5). We also demonstrated that blocking Rab11 function by either overexpression of a dominant negative form of Rab11 or knockdown of Rab11 suppressed both the translocation of ICAM-1 to the cell surface of donor cells and EBV transmission (Fig. 6).

Earlier studies demonstrated that Rab11 regulates transport of a wide variety of adhesion molecules including LFA-1, α5β1 integrin, NCAM, and E-cadherin (Desclozeaux *et al.*, 2008; Diestel *et al.*, 2007; Kelly *et al.*, 2012; Lock & Stow, 2005; Mamdouh *et al.*, 2003; Welz *et al.*, 2014). Consistent with our result (Fig. 5), some recycling NCAM and E-cadherin have been found to co-localize with Rab11 in the cytoplasm (Desclozeaux *et al.*, 2008; Kelly *et al.*, 2012; Lock & Stow, 2005). ICAM-1 appears to be recycled to the cell surface, although the involvement of Rab11 in this trafficking had not been established (Muro *et al.*, 2005). Our data indicate that EBV likely exploits the Rab11-mediated recycling of ICAM-1 for further stabilization of cell contact and subsequent viral transmission. In addition, the pattern of distribution of ICAM-1 in co-cultured BL cells (Fig. 4 and 5) was distinct from the tight distribution formed in the VS-mediated retrovirus transmission, indicating that EBV is unlikely to be transmitted in a VS-dependent manner.

Previously Shannon-Lowe and colleagues investigated the mechanism of transmission by cell-to-cell contact of EBV. In contrast to our co-culturing system, they

adsorbed cell free EBV virions to the surface of EBV-negative B cells, co-cultured these cell-bound virions with epithelial cells. They demonstrated that the majority of virions were retained on cell surfaces and that co-cultivation with epithelial cells initiated formation of CD21-mediated VS-like conjugate at the interface of contacted cells, leading to efficient EBV infection (Shannon-Lowe & Rowe, 2011; Shannon-Lowe *et al.*, 2006). The same group observed that the site of conjugation was composed of viral glycoproteins, viral receptors derived from B cells, and a variety of adhesion molecules (Shannon-Lowe & Rowe, 2011).

Multiple observations indicate that epithelial cells are likely infected *in vivo* during their intimate contact with EBV-positive B cells, a situation we reproduce with our co-culture condition. For example, it has been demonstrated that the mucosa of oropharyngeal tissue is heavily infiltrated by lymphocytes (Nagura, 1992) a site where EBV transmission is thought to occur. In addition, the atrophic border of the gastric mucosa, where EBV-associated gastric carcinoma develops, frequently generates mild to moderate atrophy and attracts inflammatory cells including lymphocytes (Hirano *et al.*, 2003). We have demonstrated that cell-to-cell contact induces the viral lytic cycle in EBV-infected BL cells (Nanbo *et al.*, 2012), indicating that it is likely that cell contact between infiltrating B cells and epithelial cells initiates the lytic cycle in B cells, which would promote the establishment of viral transmission. In accord with this idea, the lytic cycle in EBV-infected cells has been observed in secondary lymphoid tissues (Hudnall *et al.*, 2005).

These observations, along with pathological studies, suggest that transmission of EBV by cell-to-cell contact EBV transmission between latently infected B cells and

epithelial cells is an appropriate model for the establishment of persistent EBV infection in oropharyngeal tissue and/or for development of EBV-associated gastric cancer.

Several studies indicate that the direct interaction between viral glycoproteins gH/gL complex, and the αvβ5, αvβ6, and αvβ8 integrins initiate fusion of cell-free EBV and the plasma membrane of epithelial cells (Chesnokova & Hutt-Fletcher, 2011; Molesworth *et al.*, 2000). In contrast, Tugizov *et al.* demonstrated that cell-free EBV enters polarized oral epithelial cells through bidirectional transcytosis (Tugizov *et al.*, 2003), mediated either by macropinocytosis from apical to basolateral, or by caveolae-mediated endocytosis from basolateral to apical surfaces. These contrasting findings reveal that cell-free EBV enters epithelial cells *via* multiple pathways, which may reflect different receptors and cell types. Previously an EBV glycoprotein, BMRF2 was identified as a viral factor that contributes to cell-to-cell EBV transmission through interaction with α5β1, α3β1 and αvβ1 integrins (Xiao *et al.*, 2008; 2009). However, other studies indicate that BMRF2 is not required for cell-to-cell fusion (Haan *et al.*, 2001; McShane & Longnecker, 2004) and apparently very few BMRF2 molecules exist on the virion (Johannsen *et al.*, 2004), suggesting that undefined additional receptors in epithelial cells may function in the transmission of EBV mediated by cell contact.

We demonstrated that EBV is likely transmitted to Vero-E6 cells *via* clathrin-dependent endocytosis, which is facilitated by cell-to-cell contact (Fig. 7 and 8). We have also demonstrated that the neutralization antibodies for αvβ5 and αvβ6 did not block the transmission of EBV mediated by cell-to-cell contact (Fig. 2). Thus, it is unlikely that EBV transmission is established by fusion between the virus envelope and the cell membrane.

We favor a model for the transmission of EBV by cell-to-cell contact, in which the initial cell contact is established by the interaction of pre-existing adhesion molecules in BL cells and epithelial cells, resulting in the recruitment of additional adhesion molecules to the cell surface of BL cells followed by stabilization of the cell contact. The initial cell contact between BL cells and epithelial cells also up-regulates clathrin-dependent endocytosis in recipient cells, which in turn facilitates the delivery of virions to the recipient cells. Taken together, our study demonstrates that EBV exploits host the endocytic pathway for efficient viral transmission, providing new insights into the mechanism of cell-to-cell viral transmission.

Methods

Plasmids

The pEGFP-C3 plasmids encoding enhanced green fluorescent protein (eGFP)-fused wild-type Rab11 (eGFP-wtRab11) and dominant-negative form Rab11 (eGFP-Rab11 S25N) (Chen *et al.*, 1998) (were kind gifts from Dr. Angela Wandinger-Ness (University of New Mexico). The eGFP-wtRab11 and eGFP-Rab11 S25N cDNAs were cloned into a moloney murine leukemia virus-based retrovirus plasmid (Kenney, 2007) , a kind gift from Dr. Bill Sugden (University of Wisconsin-Madison). The pEGFP-N1 plasmids encoding eGFP-fused wild-type Dynamine 2 (wtDyn2-eGFP) and dominant-negative form Dynamine (Dyn2 K44A-eGFP) (Orth *et al.*, 2002) were kind gifts from Dr. Mark A, McNiven (Mayo Clinic).

Cell culture

EBV-positive and -negative African BL-derived Akata (Akata$^+$ and Akata$^-$, respectively) (Nanbo *et al.*, 2002; Shimizu *et al.*, 1994; Takada *et al.*, 1991) were maintained in RPMI-1640 medium containing 10% fetal bovine serum (FBS) (Sigma-Aldrich) and antibiotics. Akata$^-$ EBV-eGFP cells, which are latently infected with a recombinant Akata strain EBV encoding eGFP gene inserted into viral BXLF1 ORF (Maruo *et al.*, 2001a), were maintained in RPMI-1640 medium containing 10% FBS, antibiotics and 800 μg/ml G418. EBV-negative African green monkey kidney epithelial Vero-E6 cells (Desmyter *et al.*, 1968; Nanbo *et al.*, 2010; Nanbo *et al.*, 2012; Nanbo *et al.*, 2013b), which was provided by Dr. Ayato Takada (Hokkaido University), human gastric carcinoma epithelial AGS cells (Barranco *et al.*, 1983; Yoshiyama *et al.*, 1997), and human nasopharyngeal carcinoma CNE1 cells (Sizhong *et al.*, 1983) were grown in high-glucose Dulbecco's modified Eagle's medium (DMEM) containing 10% FBS and antibiotics. Cells were maintained at 37°C in 5% CO_2.

Analysis of expression of adhesion molecules

For analysis of expression of adhesion molecules, Akata$^+$, Akata$^-$, Vero-E6, AGS, or CNE1 cells (5 x 10^5, each) were incubated with mouse monoclonal antibodies for CD29 or integrin β1 subunit (clone 4B4; Beckman Coulter), CD49d or integrin α4 subunit (clone HP1/2; Beckman Coulter), CD49e or integrin α5 subunit (clone SAM1; Beckman Coulter), CD11a or integrin αL subunit (clone EP1285Y; Abcam), CD18 or integrin β2 subunit (clone 10E12; Abcam), VCAM-1 (clone STA; Abcam), Fibronectin (clone IST-3, Sigma-Aldrich), ICAM-1 (clone Ab-2; Sigma-Aldrich), αvβ5 (clone P5H9;

Beckman Coulter) or αvβ6 (clone 10D5; Abcam) for 1 h on ice. As a control, expression of estrogen receptor (ER) was analyzed with mouse anti-ER monoclonal antibody (clone TE111.5D11; Thermo Scientific). The cells were washed twice in PBS and incubated with AlexaFluor 488-labeled goat anti-mouse IgG (Life Technologies) for 30 min on ice. After washing twice in PBS, the expression of individual molecules was analyzed by flow cytometry. For the analysis of expression of adhesion moleucles in co-cultured cells, Akata^{+}, Akata^{-}, or Akata^{-} EBV-eGFP cells (2 x 10^6) were co-cultured with Vero-E6 cells (2 x 10^5) in 6-well plates for 6 h. After removal of the supernatant containing unbound cells, Akata cells that were still attached to Vero-E6 cells were removed by gentle pipetting. Vero-E6 cells were harvested by trypsinization. The expression of adhesion molecules in Akata cells and Vero-E6 cells was analyzed by flow cytometry as described above. In parallel, the harvested cells were analyzed by flow cytometry with PE-labeled monoclonal antibody for human leukocyte antigen (HLA)-DR (Sigma-Aldrich) and rabbit polyclonal antibody for caveolin-1 (Cav1) (Abcam) to confirm that harvested cells did not contain co-cultured cells.

EBV-transmission assay

Vero-E6, AGS, or CNE1 cells (5 x 10^4) were co-cultured with Akata^{-} EBV-eGFP cells (5 x 10^5) for various times in 24-well plates in the presence of absence of 1% goat anti-human IgG (DAKO). To remove the co-cultured Akata^{-} EBV-eGFP cells, individual epithelial cells were washed with the medium three times, trypsinized, and cultured in 6-well plates for 6 h. Vero-E6 cells were harvested and fixed in 4% paraformaldehyde (PFA) in PBS for 10 min at room temperature. The percentages of eGFP-positive

epithelial cells were analyzed by flow cytometry (FACSCalibur, Becton, Dickinson and company). In parallel with flow cytometric analysis, the same sample was analyzed by a confocal laser scanning microscope to confirm that the sample did not contain Akata$^-$ EBV-eGFP cells. To examine the effect of blocking antibodies to adhesion molecules on EBV transmission, Akata$^-$ EBV-eGFP cells and individual epithelial cells were separately pre-incubated with mouse monoclonal antibodies for CD29 (clone 4B4) (Martinez-Vinambres *et al.*, 2012), CD49d (clone HP1/2) (Porter & Hogg, 1997), CD49e or (clone SAM1) (Porter & Hogg, 1997), VCAM-1 (clone B-K9; Abcam) (Lefevre *et al.*, 2009), ICAM-1 (clone BBIG-I1, Beckman Coulter) (Pennino *et al.*, 2010), αvβ5 (clone P5H9) (Echevarria *et al.*, 2011), αvβ6 (clone 10D5) (Huang *et al.*, 1998), or ER (clone TE111.5D11) (Biswas *et al.*, 1998)for 30 min at 37˚C. Pre-treated cells were co-cultured in the presence of individual antibodies for 24 h and EBV transmission into epithelial cells was analyzed by flow cytometry. To determine the role of dynamin in EBV transmission, Vero-E6 cells were transfected with the expression plasmids for wtDyn2-eGFP or Dyn2 K44A-eGFP with TransIT-LT1 (Mirus). At 48 h post-transfection, the cells were co-cultured with Akata$^-$ EBV-eGFP for 24 h and EBV transmission was analyzed as described above. The expression of Dyn2 derivatives was analyzed by Western blot with rabbit anti-dynamin polyclonal antibody (clone C2C3; GeneTex).

Immunofluorescent staining

Akata$^+$ or Akata$^-$ cells (2 x 10^6) were co-cultured with Vero-E6 cells (2 x 10^5) in 35 mm glass-bottomed culture dishes (MatTek corporation) for various times. The cells were fixed with 4% PFA in PBS for 10 min at room temperature, permeabilized with

PBS containing 0.05% Triton X-100 for 10 min at room temperature and blocked in PBS containing 1% bovine serum albumin (BSA) and 0.05% Triton X-100 for 20 min at room temperature. The cells were incubated with mouse anti-ICAM-1 monoclonal antibody (clone Ab-2) and/or rabbit anti-Rab11 polyclonal antibody (Abcam) for 1 h at room temperature. After washing twice in PBS, the cells were incubated with AlexaFluor 488-labeled anti mouse IgG and/or AlexaFluor 594-labeled anti-rabbit IgG (Life Technologies) for 1 h at room temperature. After washing twice in PBS, the nuclei were counterstained with 4',6-diamidino-2-phenylindole (DAPI). Images were collected with a 60 × water-immersion objective (NA=1.3) of a confocal laser scanning microscope (Fluoview FV10i, Olympus) and acquired by using FV10-ASW software (Olympus).

Retroviral infection

Recombinant retroviruses for the expression of eGFP-wtRab11 and eGFP-Rab11 S25N were produced and purified as previously described (Nanbo *et al.*, 2010; Nanbo *et al.*, 2002; Nanbo *et al.*, 2012). For retroviral infections, Akata$^-$ EBV-eGFP cells (1 x 10^5) were grown in 24-well plates, at which point the culture medium was replaced with ice-cold MEM supplemented with 10% FBS and 20 mM Hepes (pH 7.4), and the cells were incubated with viral stocks (10^7-10^8 infectious units/ml) for 1 h at 4°C at a multiplicity of infection (m.o.i) of 5. After being washed twice with complete medium, the cells were cultured in complete medium for 48 h. The expression of eGFP-wtRab11 and eGFP-Rab11 S25N was analyzed by Western blotting with mouse monoclonal anti-Rab11 antibody (clone 47/Rab11; Beckman Coulter) at 48 hours-post infection. The effect of

expression of eGFP-wtRab11 and eGFP-Rab11 S25N on EBV transmission into Vero-E6 cells was analyzed as described for the EBV transmission assay.

siRNA treatment

Target sequences corresponding to the human Rab11a (Takahashi *et al.*, 2012), Rab11b (Moskowitz *et al.*, 2005), clathrin heavy chain (CHC), Cav1 (Manninen *et al.*, 2005), and sorting nexin 1 (SNX1) (Kerr *et al.*, 2006; Mamdouh *et al.*, 2003)-coding sequences were selected and synthesized (Life Technologies). As control, siRNAs with the target sequence against human glyceraldehyde-3-phosphate dehydrogenase (GAPDH) (Shanghai GenePharma) were used (Nanbo *et al.*, 2013a). siRNAs against Rab11a and/or Rab11b were transfected into Akata$^-$ EBV-eGFP cells (1×10^6) by electroporation (NEPA gene; 0.75 kV, 3 ms). The down-regulation of Rab11 gene was analyzed by Western blotting with mouse monoclonal anti-Rab11 antibody (clone 47/Rab11) at 48 hours-post transfection. CHC, Cav1, or SNX1 siRNAs was transfected into Vero-E6 cells (1×10^5) by using TransIT-TKO (Takara Bio). The down-regulation of individual target genes was analyzed by flow cytometric analysis with rabbit anti-CHC (Abcam), anti-Cav1 (Abcam), or anti-SNX1 polyclonal antibody (Abcam). The effect of knockdown of Rab11 isoforms in Akata$^-$ EBV-eGFP cells, and that of CHC, Cav1, or SNX1 in Vero-E6 cells on EBV transmission was analyzed as described for the EBV transmission assay.

Inhibitor treatment

To examine the effect of inhibitors on EBV transmission, Akata$^-$ EBV-eGFP cells and Vero-E6 cells were separately pre-treated with various concentration of Dynasore

(Sigma-Aldrich) or NH_4Cl (Sigma-Aldrich) for 30 min. Pre-treated cells were co-cultured in the presence of inhibitors for 24 h and EBV transmission was analyzed as described above. For analysis of the effect of the inhibitors on induction of lytic cycle, Vero-E6 cells were co-cultured with Akata$^+$ cells treated with 1% αhIgG in the presence of 1 μM Dynasore or 20 mM NH_4Cl for 24 h. Akata$^+$ cells were harvested, fixed, permeabilized and blocked as described above. The cells were incubated with anti-gp350 monoclonal antibody (C-1) (Thorley-Lawson & Geilinger, 1980) for 1 h at room temperature, washed twice in PBS, and incubated with AlexaFluor 488-labeled secondary antibody. After washing twice in PBS, the expression of gp350 was analyzed by a flow cytometry.

Transferrin uptake assays

Akata$^+$ or Akata$^-$ cells were co-cultured with control or CHC siRNAs transfected- Vero-E6 cells for 6 h at 37°C. Co-cultured cells were further incubated in the presence of 2 μg/ml AlexaFluor 594-labeled Transferrin (Life Technologies) for 10 min at 37°C. Vero-E6 cells were harvested by trypsin and fixed with 4% PFA. The efficiency of uptake of transferrin was analyzed by use of flow cytometry.

Acknowledgement

We acknowledge Drs Ayato Takada (Hokkaido University), Angela Wandinger-Ness (University of New Mexico), Mark A, McNiven (Mayo Clinic) and Bill Sugden (University of Wisconsin, Madison) with Vero-E6 cells, expression plasmids for eGFP-wtRab11 and eGFP-Rab11 S25N, expression plasmids for wtDyn2-eGFP and Dyn2

K44A-eGFP, and a retrovirus plasmid, respectively. We also thank Dr. Bill Sugden for critically reviewing the manuscript. This work was supported by grants-in-aid from the Japanese Ministry of Education, Science, Sports, Culture, and Technology, Japan and Takeda Science Foundation.

References

Agosto, L. M., Uchil, P. D. & Mothes, W. (2015). HIV cell-to-cell transmission: effects on pathogenesis and antiretroviral therapy. *Trends Microbiol* **23**, 289-295.

Barranco, S. C., Townsend, C. M., Jr., Casartelli, C., Macik, B. G., Burger, N. L., Boerwinkle, W. R. & Gourley, W. K. (1983). Establishment and characterization of an in vitro model system for human adenocarcinoma of the stomach. *Cancer Res* **43**, 1703-1709.

Biswas, D. K., Averboukh, L., Sheng, S., Martin, K., Ewaniuk, D. S., Jawde, T. F., Wang, F. & Pardee, A. B. (1998). Classification of breast cancer cells on the basis of a functional assay for estrogen receptor. *Mol Med* **4**, 454-467.

Bosch, B., Grigorov, B., Senserrich, J., Clotet, B., Darlix, J. L., Muriaux, D. & Este, J. A. (2008). A clathrin-dynamin-dependent endocytic pathway for the uptake of HIV-1 by direct T cell-T cell transmission. *Antiviral Res* **80**, 185-193.

Chang, Y., Tung, C. H., Huang, Y. T., Lu, J., Chen, J. Y. & Tsai, C. H. (1999). Requirement for cell-to-cell contact in Epstein-Barr virus infection of nasopharyngeal carcinoma cells and keratinocytes. *J Virol* **73**, 8857-8866.

Chen, W., Feng, Y., Chen, D. & Wandinger-Ness, A. (1998). Rab11 is required for trans-golgi network-to-plasma membrane transport and a preferential target for GDP dissociation inhibitor. *Mol Biol Cell* **9**, 3241-3257.

Chesnokova, L. S. & Hutt-Fletcher, L. M. (2011). Fusion of Epstein-Barr virus with epithelial cells can be triggered by alphavbeta5 in addition to alphavbeta6 and alphavbeta8, and integrin binding triggers a conformational change in glycoproteins gHgL. *J Virol* **85**, 13214-13223.

Couet, J., Belanger, M. M., Roussel, E. & Drolet, M. C. (2001). Cell biology of caveolae and caveolin. *Adv Drug Deliv Rev* **49**, 223-235.

Dale, B. M., McNerney, G. P., Thompson, D. L., Hubner, W., de Los Reyes, K., Chuang, F. Y., Huser, T. & Chen, B. K. (2011). Cell-to-cell transfer of HIV-1 via virological synapses leads to endosomal virion maturation that activates viral membrane fusion. *Cell Host Microbe* **10**, 551-562.

Desclozeaux, M., Venturato, J., Wylie, F. G., Kay, J. G., Joseph, S. R., Le, H. T. & Stow, J. L. (2008). Active Rab11 and functional recycling endosome are required for E-cadherin trafficking and lumen formation during epithelial morphogenesis. *Am J Physiol Cell Physiol* **295**, C545-556.

Desmyter, J., Melnick, J. L. & Rawls, W. E. (1968). Defectiveness of interferon production and of rubella virus interference in a line of African green monkey kidney cells (Vero). *J Virol* **2**, 955-961.

Diestel, S., Schaefer, D., Cremer, H. & Schmitz, B. (2007). NCAM is ubiquitylated, endocytosed and recycled in neurons. *J Cell Sci* **120**, 4035-4049.

Echevarria, T. J., Chow, S., Watson, S., Wakefield, D. & Di Girolamo, N. (2011). Vitronectin: a matrix support factor for human limbal epithelial progenitor cells. *Invest Ophthalmol Vis Sci* **52**, 8138-8147.

Fingeroth, J. D., Diamond, M. E., Sage, D. R., Hayman, J. & Yates, J. L. (1999). CD21-Dependent infection of an epithelial cell line, 293, by Epstein-Barr virus. *J Virol* **73**, 2115-2125.

Gilbert, C., Cantin, R., Barat, C. & Tremblay, M. J. (2007). Human immunodeficiency virus type 1 replication in dendritic cell-T-cell cocultures is increased upon incorporation of host LFA-1 due to higher levels of virus production in immature dendritic cells. *J Virol* **81**, 7672-7682.

Gromov, P. S., Celis, J. E., Hansen, C., Tommerup, N., Gromova, I. & Madsen, P. (1998). Human rab11a: transcription, chromosome mapping and effect on the expression levels of host GTP-binding proteins. *FEBS Lett* **429**, 359-364.

Groot, F., Kuijpers, T. W., Berkhout, B. & de Jong, E. C. (2006). Dendritic cell-mediated HIV-1 transmission to T cells of LAD-1 patients is impaired due to the defect in LFA-1. *Retrovirology* **3**, 75.

Gummuluru, S., KewalRamani, V. N. & Emerman, M. (2002). Dendritic cell-mediated viral transfer to T cells is required for human immunodeficiency virus type 1 persistence in the face of rapid cell turnover. *J Virol* **76**, 10692-10701.

Haan, K. M., Lee, S. K. & Longnecker, R. (2001). Different functional domains in the cytoplasmic tail of glycoprotein B are involved in Epstein-Barr virus-induced membrane fusion. *Virology* **290**, 106-114.

Hioe, C. E., Chien, P. C., Jr., Lu, C., Springer, T. A., Wang, X. H., Bandres, J. & Tuen, M. (2001). LFA-1 expression on target cells promotes human immunodeficiency virus type 1 infection and transmission. *J Virol* **75**, 1077-1082.

Hirano, A., Yanai, H., Shimizu, N., Okamoto, T., Matsubara, Y., Yamamoto, K. & Okita, K. (2003). Evaluation of epstein-barr virus DNA load in gastric mucosa with chronic atrophic gastritis using a real-time quantitative PCR assay. *Int J Gastrointest Cancer* **34**, 87-94.

Huang, X., Wu, J., Spong, S. & Sheppard, D. (1998). The integrin alphavbeta6 is critical for keratinocyte migration on both its known ligand, fibronectin, and on vitronectin. *J Cell Sci* **111 (Pt 15)**, 2189-2195.

Hudnall, S. D., Ge, Y., Wei, L., Yang, N. P., Wang, H. Q. & Chen, T. (2005). Distribution and phenotype of Epstein-Barr virus-infected cells in human pharyngeal tonsils. *Mod Pathol* **18**, 519-527.

Iizasa, H., Nanbo, A., Nishikawa, J., Jinushi, M. & Yoshiyama, H. (2012). Epstein-Barr Virus (EBV)-associated gastric carcinoma. *Viruses* **4**, 3420-3439.

Imai, S., Nishikawa, J. & Takada, K. (1998). Cell-to-cell contact as an efficient mode of Epstein-Barr virus infection of diverse human epithelial cells. *J Virol* **72**, 4371-4378.

Johannsen, E., Luftig, M., Chase, M. R., Weicksel, S., Cahir-McFarland, E., Illanes, D., Sarracino, D. & Kieff, E. (2004). Proteins of purified Epstein-Barr virus. *Proc Natl Acad Sci U S A* **101**, 16286-16291.

Jolly, C., Kashefi, K., Hollinshead, M. & Sattentau, Q. J. (2004). HIV-1 cell to cell transfer across an Env-induced, actin-dependent synapse. *J Exp Med* **199**, 283-293.

Jolly, C., Mitar, I. & Sattentau, Q. J. (2007). Adhesion molecule interactions facilitate human immunodeficiency virus type 1-induced virological synapse formation between T cells. *J Virol* **81**, 13916-13921.

Jolly, C. & Sattentau, Q. J. (2004). Retroviral spread by induction of virological synapses. *Traffic* **5**, 643-650.

Kelly, E. E., Horgan, C. P. & McCaffrey, M. W. (2012). Rab11 proteins in health and disease. *Biochem Soc Trans* **40**, 1360-1367.

Kenney, S. C. (2007). Reactivation and lytic replication of EBV.

Kerr, M. C., Lindsay, M. R., Luetterforst, R., Hamilton, N., Simpson, F., Parton, R. G., Gleeson, P. A. & Teasdale, R. D. (2006). Visualisation of macropinosome maturation by the recruitment of sorting nexins. *J Cell Sci* **119**, 3967-3980.

Kieff, E. & Rickinson, A. B. (2001). Epstein-Barr virus and its replication. *In M Knipe and P M Howley (ed), Fields virology, 4th ed Lippincott Williams & Wilkins, Philadelphia, PA*, 2511-2573.

Lefevre, S., Knedla, A., Tennie, C., Kampmann, A., Wunrau, C., Dinser, R., Korb, A., Schnaker, E. M., Tarner, I. H., Robbins, P. D., Evans, C. H., Sturz, H., Steinmeyer, J., Gay, S., Scholmerich, J., Pap, T., Muller-Ladner, U. & Neumann, E. (2009). Synovial fibroblasts spread rheumatoid arthritis to unaffected joints. *Nat Med* **15**, 1414-1420.

Li, Q., Spriggs, M. K., Kovats, S., Turk, S. M., Comeau, M. R., Nepom, B. & Hutt-Fletcher, L. M. (1997). Epstein-Barr virus uses HLA class II as a cofactor for infection of B lymphocytes. *J Virol* **71**, 4657-4662.

Lock, J. G. & Stow, J. L. (2005). Rab11 in recycling endosomes regulates the sorting and basolateral transport of E-cadherin. *Mol Biol Cell* **16**, 1744-1755.

Mamdouh, Z., Chen, X., Pierini, L. M., Maxfield, F. R. & Muller, W. A. (2003). Targeted recycling of PECAM from endothelial surface-connected compartments during diapedesis. *Nature* **421**, 748-753.

Manninen, A., Verkade, P., Le Lay, S., Torkko, J., Kasper, M., Fullekrug, J. & Simons, K. (2005). Caveolin-1 is not essential for biosynthetic apical membrane transport. *Mol Cell Biol* **25**, 10087-10096.

Martinez-Vinambres, E., Garcia-Trujillo, J. A., Rodriguez-Martin, E., Villar, L. M., Coll, J. & Roldan, E. (2012). CD29 expressed on plasma cells is activated by divalent cations and soluble CD106 contained in the bone marrow plasma: refractory activation is associated with enhanced proliferation and exit of clonal plasma cells to circulation in multiple myeloma patients. *Leukemia* **26**, 1098-1105.

Maruo, S., Nanbo, A. & Takada, K. (2001a). Replacement of the Epstein-Barr virus plasmid with the EBER plasmid in Burkitt's lymphoma cells. *J Virol* **75**, 9977-9982.

Maruo, S., Yang, L. & Takada, K. (2001b). Roles of Epstein-Barr virus glycoproteins gp350 and gp25 in the infection of human epithelial cells. *J Gen Virol* **82**, 2373-2383.

McShane, M. P. & Longnecker, R. (2004). Cell-surface expression of a mutated Epstein-Barr virus glycoprotein B allows fusion independent of other viral proteins. *Proc Natl Acad Sci U S A* **101**, 17474-17479.

Molesworth, S. J., Lake, C. M., Borza, C. M., Turk, S. M. & Hutt-Fletcher, L. M. (2000). Epstein-Barr virus gH is essential for penetration of B cells but also plays a role in attachment of virus to epithelial cells. *J Virol* **74**, 6324-6332.

Moskowitz, H. S., Yokoyama, C. T. & Ryan, T. A. (2005). Highly cooperative control of endocytosis by clathrin. *Mol Biol Cell* **16**, 1769-1776.

Muro, S., Gajewski, C., Koval, M. & Muzykantov, V. R. (2005). ICAM-1 recycling in endothelial cells: a novel pathway for sustained intracellular delivery and prolonged effects of drugs. *Blood* **105**, 650-658.

Nagura, H. (1992). Mucosal defense mechanism in health and disease. Role of the mucosal immune system. *Acta Pathol Jpn* **42**, 387-400.

Nanbo, A., Imai, M., Watanabe, S., Noda, T., Takahashi, K., Neumann, G., Halfmann, P. & Kawaoka, Y. (2010). Ebolavirus is internalized into host cells via macropinocytosis in a viral glycoprotein-dependent manner. *PLoS Pathog* **6**, e1001121.

Nanbo, A., Inoue, K., Adachi-Takasawa, K. & Takada, K. (2002). Epstein-Barr virus RNA confers resistance to interferon-alpha-induced apoptosis in Burkitt's lymphoma. *EMBO J* **21**, 954-965.

Nanbo, A., Kawanishi, E., Yoshida, R. & Yoshiyama, H. (2013a). Exosomes derived from Epstein-Barr virus-infected cells are internalized via caveola-dependent endocytosis and promote phenotypic modulation in target cells. *J Virol* **87**, 10334-10347.

Nanbo, A., Terada, H., Kachi, K., Takada, K. & Matsuda, T. (2012). Roles of cell signaling pathways in cell-to-cell contact-mediated Epstein-Barr virus transmission. *J Virol* **86**, 9285-9296.

Nanbo, A., Watanabe, S., Halfmann, P. & Kawaoka, Y. (2013b). The spatio-temporal distribution dynamics of Ebola virus proteins and RNA in infected cells. *Sci Rep* **3**, 1206.

Nemerow, G. R., Mold, C., Schwend, V. K., Tollefson, V. & Cooper, N. R. (1987). Identification of gp350 as the viral glycoprotein mediating attachment of Epstein-Barr virus (EBV) to the EBV/C3d receptor of B cells: sequence homology of gp350 and C3 complement fragment C3d. *J Virol* **61**, 1416-1420.

Newton, A. J., Kirchhausen, T. & Murthy, V. N. (2006). Inhibition of dynamin completely blocks compensatory synaptic vesicle endocytosis. *Proc Natl Acad Sci U S A* **103**, 17955-17960.

Oda, T., Imai, S., Chiba, S. & Takada, K. (2000). Epstein-Barr virus lacking glycoprotein gp85 cannot infect B cells and epithelial cells. *Virology* **276**, 52-58.

Orth, J. D., Krueger, E. W., Cao, H. & McNiven, M. A. (2002). The large GTPase dynamin regulates actin comet formation and movement in living cells. *Proc Natl Acad Sci U S A* **99**, 167-172.

Pennino, D., Eyerich, K., Scarponi, C., Carbone, T., Eyerich, S., Nasorri, F., Garcovich, S., Traidl-Hoffmann, C., Albanesi, C. & Cavani, A. (2010). IL-17 amplifies human contact hypersensitivity by licensing hapten nonspecific Th1 cells to kill autologous keratinocytes. *J Immunol* **184**, 4880-4888.

Porter, J. C. & Hogg, N. (1997). Integrin cross talk: activation of lymphocyte function-associated antigen-1 on human T cells alters alpha4beta1- and alpha5beta1-mediated function. *J Cell Biol* **138**, 1437-1447.

Puigdomenech, I., Massanella, M., Cabrera, C., Clotet, B. & Blanco, J. (2009). On the steps of cell-to-cell HIV transmission between CD4 T cells. *Retrovirology* **6**, 89.

Ren, M., Xu, G., Zeng, J., De Lemos-Chiarandini, C., Adesnik, M. & Sabatini, D. D. (1998). Hydrolysis of GTP on rab11 is required for the direct delivery of transferrin from the pericentriolar recycling compartment to the cell surface but not from sorting endosomes. *Proc Natl Acad Sci U S A* **95**, 6187-6192.

Shannon-Lowe, C. & Rowe, M. (2011). Epstein-Barr virus infection of polarized epithelial cells via the basolateral surface by memory B cell-mediated transfer infection. *PLoS Pathog* **7**, e1001338.

Shannon-Lowe, C. D., Neuhierl, B., Baldwin, G., Rickinson, A. B. & Delecluse, H. J. (2006). Resting B cells as a transfer vehicle for Epstein-Barr virus infection of epithelial cells. *Proc Natl Acad Sci U S A* **103**, 7065-7070.

Shimizu, N., Tanabe-Tochikura, A., Kuroiwa, Y. & Takada, K. (1994). Isolation of Epstein-Barr virus (EBV)-negative cell clones from the EBV-positive Burkitt's lymphoma (BL) line Akata: malignant phenotypes of BL cells are dependent on EBV. *J Virol* **68**, 6069-6073.

Silvis, M. R., Bertrand, C. A., Ameen, N., Golin-Bisello, F., Butterworth, M. B., Frizzell, R. A. & Bradbury, N. A. (2009). Rab11b regulates the apical recycling of the cystic fibrosis transmembrane conductance regulator in polarized intestinal epithelial cells. *Mol Biol Cell* **20**, 2337-2350.

Sizhong, Z., Xiukung, G. & Yi, Z. (1983). Cytogenetic studies on an epithelial cell line derived from poorly differentiated nasopharyngeal carcinoma. *Int J Cancer* **31**, 587-590.

Speck, P. & Longnecker, R. (2000). Infection of breast epithelial cells with Epstein-Barr virus via cell-to-cell contact. *J Natl Cancer Inst* **92**, 1849-1851.

Takada, K. (1984). Cross-linking of cell surface immunoglobulins induces Epstein-Barr virus in Burkitt lymphoma lines. *Int J Cancer* **33**, 27-32.

Takada, K., Horinouchi, K., Ono, Y., Aya, T., Osato, T., Takahashi, M. & Hayasaka, S. (1991). An Epstein-Barr virus-producer line Akata: establishment of the cell line and analysis of viral DNA. *Virus Genes* **5**, 147-156.

Takada, K. & Ono, Y. (1989). Synchronous and sequential activation of latently infected Epstein-Barr virus genomes. *J Virol* **63**, 445-449.

Takahashi, S., Kubo, K., Waguri, S., Yabashi, A., Shin, H. W., Katoh, Y. & Nakayama, K. (2012). Rab11 regulates exocytosis of recycling vesicles at the plasma membrane. *J Cell Sci* **125**, 4049-4057.

Tanner, J., Weis, J., Fearon, D., Whang, Y. & Kieff, E. (1987). Epstein-Barr virus gp350/220 binding to the B lymphocyte C3d receptor mediates adsorption, capping, and endocytosis. *Cell* **50**, 203-213.

Tanner, J., Whang, Y., Sample, J., Sears, A. & Kieff, E. (1988). Soluble gp350/220 and deletion mutant glycoproteins block Epstein-Barr virus adsorption to lymphocytes. *J Virol* **62**, 4452-4464.

Tardif, M. R. & Tremblay, M. J. (2003). Presence of host ICAM-1 in human immunodeficiency virus type 1 virions increases productive infection of CD4+ T lymphocytes by favoring cytosolic delivery of viral material. *J Virol* **77**, 12299-12309.

Tardif, M. R. & Tremblay, M. J. (2005). LFA-1 is a key determinant for preferential infection of memory CD4+ T cells by human immunodeficiency virus type 1. *J Virol* **79**, 13714-13724.

Thorley-Lawson, D. A. & Geilinger, K. (1980). Monoclonal antibodies against the major glycoprotein (gp350/220) of Epstein-Barr virus neutralize infectivity. *Proc Natl Acad Sci U S A* **77**, 5307-5311.

Trowsdale, J., Ragoussis, J. & Campbell, R. D. (1991). Map of the human MHC. *Immunol Today* **12**, 443-446.

Tugizov, S. M., Herrera, R. & Palefsky, J. M. (2003). Epstein-Barr virus transcytosis through polarized oral epithelial cells. *J Virol* **87**, 8179-8194.

Wang, J. H., Kwas, C. & Wu, L. (2009). Intercellular adhesion molecule 1 (ICAM-1), but not ICAM-2 and -3, is important for dendritic cell-mediated human immunodeficiency virus type 1 transmission. *J Virol* **83**, 4195-4204.

Welz, T., Wellbourne-Wood, J. & Kerkhoff, E. (2014). Orchestration of cell surface proteins by Rab11. *Trends Cell Biol* **24**, 407-415.

Xiao, J., Palefsky, J. M., Herrera, R., Berline, J. & Tugizov, S. M. (2008). The Epstein-Barr virus BMRF-2 protein facilitates virus attachment to oral epithelial cells. *Virology* **370**, 430-442.

Xiao, J., Palefsky, J. M., Herrera, R., Berline, J. & Tugizov, S. M. (2009). EBV BMRF-2 facilitates cell-to-cell spread of virus within polarized oral epithelial cells. *Virology* **388**, 335-343.

Yoshiyama, H., Imai, S., Shimizu, N. & Takada, K. (1997). Epstein-Barr virus infection of human gastric carcinoma cells: implication of the existence of a new virus receptor different from CD21. *J Virol* **71**, 5688-5691.

Zhong, P., Agosto, L. M., Munro, J. B. & Mothes, W. (2013). Cell-to-cell transmission of viruses. *Curr Opin Virol* **3**, 44-50.

Figure Legends

Fig. 1. Expression of adhesion molecules in Akata cells and epithelial cells.

Akata^{+} cells (a), Akata^{-} cells (b), Vero-E6 cells (c), AGS cells (d), or CNE1 cells (e) were incubated with antibodies for CD49d, CD49e, CD29, CD11a, CD18, VCAM-1, fibronectin, ICAM-1, αvβ5, αvβ6, or ER. The expression of individual molecules was revealed with AlexaFluor 488-labeled secondary antibodies (boldface lines) by flow cytometry. As a control, cells were incubated with the secondary antibody (thin lines). The experiments were performed three times independently and representative histograms are presented.

Fig. 2. Effect of neutralizing antibodies on cell-to-cell EBV transmission

(a) EBV-eGFP is transmitted to various epithelial cells. Vero-E6, AGS or CNE1 cells were co-cultured with Akata^{-}EBV-eGFP cells in the absence or presence of αhIgG for 24 h to induce EBV's productive cycle. The percentages of eGFP-positive, infected epithelial cells were analyzed by flow cytometry. The experiment was performed three times independently and the average values and their standard deviations are shown for each condition. (b) The effect of blocking antibodies on cell-to-cell contact-mediated EBV transmission into Vero-E6 cells. Akata^{-} EBV-eGFP cells were treated with (grey bars) or without (white bars) 1% αhIgG for 2 h at 37˚C and washed with medium. Akata^{-} EBV-eGFP cells or Vero-E6 cells were pretreated with various amounts of blocking antibodies for CD49d, CD49e, CD29, VCAM-1, ICAM-1, αvβ5, αvβ6 or ER (0.1, 0.2, 0.5, 1.0, 10 μg/ml) for 30 min for 37˚C. Pre-treated cells were co-cultured for 24 h in the

presence of individual antibodies. The percentages of EBV-eGFP-positively infected Vero-E6 cells were analyzed by flow cytometry. The infection efficiency is shown relative to the value when co-cultured with αhIgG-untreated Akata$^-$ EBV-eGFP cells in the absence of antibodies. The experiment was performed three times independently and the average and its standard deviation are shown in each condition. *, $P < 0.05$ versus respective control. **, $P < 0.01$ versus respective control (Student's *t* test). (c) The effect of neutralizing antibodies on cell-to-cell contact-mediated EBV transmission into AGS and CEN1 cells. Akata$^-$ EBV-eGFP cells were treated with 1% αhIgG for 2 h at 37˚C and washed with medium. Akata$^-$ EBV-eGFP cells, and AGS cells (gray bars) or CNE1 cells (white bars) were pretreated with various amounts of blocking antibodies for 30 min for 37˚C. Pre-treated cells were co-cultured for 24 h in the presence of individual antibodies. The percentages of EBV-eGFP-infected individual epithelial cells were analyzed by flow cytometry. The infection efficiency is shown relative to the value when cells were co-cultured Akata$^-$ EBV-eGFP cells in the absence of antibodies. The experiment was performed three times independently and the average values and their standard deviations are shown for each condition. *, $P < 0.05$ versus respective control. **, $P < 0.01$ versus respective control (Student's *t* test).

Fig. 3. Effect of cell-to-cell contact on expression of adhesion molecules in co-cultured cells

(a and b) Expression of HLA-DR and Cav1 in co-cultured cells. Akata$^+$ cells or Akata$^-$ cells were co-cultured with (boldface line) or without (dashed line) Vero-E6 cells for 24 h and expression of HLA-DR (a) or Cav1 (b) in Akata$^+$ cells (top, left), Akata$^-$ cells (top,

right) was analyzed by flow cytometry. Expression of HLA-DR (a) or Cav1 (b) in Vero-E6 cells co-cultured with (boldface line) or without (dashed line) Akata^{+} cells (bottom, left) or Akata^{-} cells (bottom, right) was analyzed by flow cytometry. As a control, cells were incubated with secondary antibodies (shadowed histogram). Representative histograms are shown. (c) Expression of HLA-DR in co-cultured cells. Akata^{+} or Akata^{-} cells were co-cultured with Vero-E6 cells for 24 h. Expression of HLA-DR in Akata^{+} cells (white bars), Akata^{-} cells (grey bars) was analyzed by flow cytometry (left). Expression of HLA-DR in Vero-E6 cells co-cultured with Akata^{+} cells (white bars) or Akata^{-} cells (grey bars) was analyzed by flow cytometry (right). The data were normalized to the expression of HLA-DR in Akata cells without cell contact. The experiment was performed three times independently and the average values and their standard deviations are shown for each condition. **, $P < 0.01$ versus respective control. n.s., not significant (Student's *t* test). (d) Expression of Cav1 in co-cultured cells. Akata^{+} or Akata^{-} cells were co-cultured with Vero-E6 cells for 24 h. Expression of Cav1 in Akata^{+} cells (white bars), Akata^{-} cells (grey bars) was analyzed by flow cytometry (left). Expression of Cav1 in Vero-E6 cells co-cultured with Akata^{+} cells (white bars) or Akata^{-} cells (grey bars) was analyzed by flow cytometry (right). The data were normalized to the expression of Cav1 in Vero-E6 without cell contact. (e and f). Effect of cell-cell contact on expression of adhesion molecule in co-cultured cells. Akata^{+} cells or Akata^{-} cells were co-cultured with (boldface line) or without (dashed line) Vero-E6 cells for 6 h. Expression of individual molecules was analyzed by flow cytometry in Akata^{+} cells (left), Akata^{-} cells (right) (e), and Vero-E6 cells co-cultured with Akata^{+} cells (left) or Akata^{-} cells (right) (f). As a control, cells were incubated with secondary antibodies (shadowed

histogram). Representative histograms are shown. (g and h) Effect of cell-cell contact on expression of adhesion molecule in co-cultured cells. Akata$^+$ cells or Akata$^-$ cells were co-cultured with Vero-E6 cells for 6 h. Expression of individual molecules was analyzed by flow cytometry in Akata$^+$ cells (white bars), Akata$^-$ cells (grey bars) (g), and Vero-E6 cells co-cultured with Akata$^+$ cells (white bars) or Akata$^-$ cells (grey bars) (h). The data are normalized to the expression of individual molecules in the cells without cell contact. The experiment was performed three times independently and the average values and their standard deviations are shown for each condition. *, $P < 0.05$ versus respective control. **, $P < 0.01$ versus respective control (Student's *t* test).

Fig. 4. Effect of cell-to-cell contact on distribution of ICAM-1 in co-cultured cells

(a and b) The kinetics of ICAM-1 expression in co-cultured cells. Akata$^+$ cells or Akata$^-$ cells were co-cultured with Vero-E6 cells for various times. The expression of ICAM-1 was analyzed by flow cytometry in Akata$^+$ cells (left), Akata$^-$ cells (right) (a) and Vero-E6 cells were co-cultured with Akata$^+$ cells (left) and Akata$^-$ cells (right) (b). The data were normalized to the expression of ICAM-1 in the cells without cell contact. As a control, cells were incubated with secondary antibodies (shadowed histogram). Representative histograms are shown. (c and d) The kinetics of ICAM-1 expression in co-cultured cells. Akata$^+$ or Akata$^-$ cells were co-cultured with Vero-E6 cells for various times. The expression of ICAM-1 was analyzed by flow cytometry in Akata$^+$ cells (white bars), Akata$^-$ cells (grey bars) (c) and Vero-E6 cells were co-cultured with Akata$^+$ cells (white bars) and Akata$^-$ cells (grey bars) (d). The data were normalized to the expression of ICAM-1 in the cells without cell contact. The experiment was performed three times

independently and the average values and their standard deviations are shown for each condition. *, $P < 0.05$ versus respective control. **, $P < 0.01$ versus respective control (Student's *t* test). (e-h) The distribution of ICAM-1 in co-cultured cells. Akata$^+$ or Akata$^-$ cells were co-cultured with Vero-E6 cells for 2, 6 and 24 h. The distribution of ICAM-1 in Akata$^+$ (e), Akata$^-$ cells (f), and Vero-E6 cells co-cultured with Akata$^+$ cells (g) and Akata$^-$ cells (h) was examined by immunofluorescent staining (top). As a control, the distribution of ICAM-1 without cell contact is shown. The nucleus was counterstained with DAPI (middle). DIC images are shown at the bottom. Scale bars, 10 μm.

Fig. 5. The distribution of ICAM-1 and of recycling endosomes in co-cultured Akata cells

(a and b) The distribution of Rab11 in co-cultured Akata cells. Akata$^+$ cells or Akata$^-$ cells were co-cultured with Vero-E6 cells for 1 h. The distributions of ICAM-1 (left, green) and of Rab11 (middle, red) in Akata$^+$ (a) and Akata$^-$ cells (b) were examined by immunofluorescent staining (bottom). As a control, the distributions of ICAM-1 and of Rab11 in the cells without cell contact were analyzed (top). The nuclei were counterstained with DAPI. Scale bars, 5 μm. (c) Z-stack images of distribution of ICAM-1 and Rab11 in co-cultured Akata$^+$ cells. Akata$^+$ cells were co-cultured with Vero-E6 cells for 1 h. The distributions of ICAM-1 (green) and Rab11 (red) in co-cultured cells were determined by immunofluorescent staining in a series of Z-stack images that were collected at 0.7 μm intervals. The nucleus was counterstained with DAPI. Scale bar, 10 μm.

Fig. 6. Role of recycling endosomes in the transmission of EBV mediated by cell-to-cell contact.

(a) Expression of wild-type Rab11 (wtRab11) and a dominant negative form of Rab11 (Rab11 N25S) in Akata$^-$ EBV-eGFP cells. eGFP-fused wtRab11 or Rab11 N25S were expressed in Akata$^-$ EBV-eGFP cells with a retrovirus vector. As a control, Akata$^-$ EBV-eGFP cells were transduced with a retrovirus vector encoding eGFP gene. The expression of eGFP-wtRab11 or -Rab11 N25S was analyzed by a Western blot at 48 h post-infection (top). As an internal control, the expression of β-actin is shown (bottom). (b) The effect of expression of eGFP-Rab11 N25S on the expression of ICAM-1 in donor cells. eGFP-fused wtRab11 or Rab11 N25S were expressed in Akata$^-$ EBV-eGFP cells with a retrovirus vector. The expression of ICAM-1 in Akata$^+$ cells expressing wtRab11 (boldface line) or Rab11 N25S (thin line) was analyzed by flow cytometry. As a control, Akata$^-$ EBV-eGFP cells were transduced with a control plasmid (dashed line). Representative histograms are shown. (c) The effect of expression of eGFP-Rab11 N25S on the distribution of ICAM-1 in donor cells. eGFP-fused wtRab11 or Rab11 N25S were expressed in Akata$^-$ EBV-eGFP cells with a retrovirus vector. The expression of ICAM-1 in Akata$^-$ EBV-eGFP was analyzed by flow cytometry. The data were normalized to the expression of ICAM-1 in the cells without cell contact. The experiment was performed three times independently and the average values and their standard deviation are shown for each condition. **, $P < 0.01$ versus respective control (Student's *t* test). (d) The effect of expression of eGFP-Rab11 N25S on the transmission of EBV mediated by cell-to-cell contact. eGFP-fused wtRab11 or Rab11 N25S were expressed in Akata$^-$ EBV-eGFP by a retrovirus vector. At 48 h post-infection, Akata$^-$ EBV-eGFP cells were co-cultured with

Vero-E6 for 24 h. The percentages of eGFP-expressing Vero-E6 cells were analyzed by flow cytometry. The data are normalized to eGFP-expression in Vero-E6 cells that were co-cultured with Akata$^-$ EBV-eGFP cells that were transduced with a retrovirus vector encoding eGFP gene. The experiment was performed three times independently and the average values and their standard deviations are shown for each condition. *, $P < 0.05$ versus respective control (Student's *t* test). (e) Knock down of Rab11 in Akata$^-$ EBV-eGFP cells. Akata$^-$ EBV-eGFP cells were transfected with control siRNA, Rab11a and/or Rab11b siRNA. Down regulation of Rab11 was analyzed with a Western blot (top) at 48 h post-transfection. As an internal control, the expression of β-actin is shown (bottom). (f) The effect of knock down of Rab11 on EBV transmission mediated by cell-to-cell contact. Akata$^-$ EBV-eGFP cells were transfected with control siRNA, Rab11a and/or Rab11b siRNA. At 48 h post-transfection, siRNA-treated Akata$^-$ EBV-eGFP cells were co-cultured with Vero-E6 cells for 24 h. The percentages of eGFP-expressing Vero-E6 cells were analyzed by flow cytometry. The data are normalized to eGFP expression in Vero-E6 cells that were co-cultured with control, siRNA-treated, Akata$^-$ EBV-eGFP cells. The experiment was performed three times independently and the average values and their standard deviations are shown for each condition. **, $P < 0.01$ versus respective control (Student's *t* test).

Fig. 7. Role of dynamine-dependent endocytosis in cell-to-cell EBV transmission

(a) The effect of dynasore on cell-to-cell EBV transmission. Vero-E6 cells were pretreated with various concentrations of dynasore for 30 min at 37°C. Akata$^-$ EBV-eGFP cells were co-cultured with Vero-E6 cells for 24 h in the presence of dynasore. (b) The

expression of wild-type dynamine 2 (wtDyn2) and a dominant negative form of Dyn 2 (Dyn2 K44A) in Vero-E6. wtDyn2-eGFP or Dyn2 K44A-eGFP were expressed in Vero-E6 cells. As a control, Vero-E6 cells were transfected with pEGFP-N1 plasmid. The expression of wtDyn2-eGFP or of Dyn2 K44A-eGFP was analyzed with a Western blot at 48 h post-infection (top). As an internal control, the expression of β-actin is shown (bottom). (c) The effect of expression of wtDyn2-eGFP and Dyn2 K44A-eGFP on EBV transmission mediated by cell-to-cell contact. Vero-E6 cells were transfected with expression plasmids for wtDyn2-eGFP and Dyn2 K44A-eGFP. At 48 h post-transfection, Vero-E6 cells were co-cultured with Akata$^-$ EBV-eGFP cells for 24 h. (d) The effect of NH_4Cl on EBV transmission mediated by cell-to-cell contact. Vero-E6 cells were pretreated with various concentrations of NH_4Cl for 30 min at 37°C. Akata$^-$ EBV-eGFP cells were co-cultured with Vero-E6 cells for 24 h in the presence of NH_4Cl. The percentages of eGFP-expressing Vero-E6 cells were analyzed by flow cytometry. The data were normalized to eGFP expression in co-cultured Vero-E6 cells that were treated with DMSO (a and d) and that were transfected with a control plasmid (c). The experiment was performed three times independently and the average values and their standard deviations are shown for each condition. *, $P < 0.05$ versus he respective control. **, $P < 0.01$ versus respective control (Student's *t* test). (e) The effect of the inhibitors on EBV replication. Akata$^-$EBV-eGFP cells that were treated or untreated with αhIgG were incubated with DMSO, Dynasore, or NH_4Cl for 24 h. The expression of gp350 was analyzed by flow cytometry. The data were normalized to αhIgG-untreated and DMSO-treated cells (bottom). The experiment was performed three times independently and the

average values and their standard deviations are shown for each condition. **, $P < 0.01$ versus respective control. n.s., not significant.

Fig. 8. Role of clathrin-dependent endocytosis in EBV transmission mediated by cell-to-cell contact

(a) Efficiency of knock down of target genes in Vero-E6 cells. Vero-E6 cells were transfected with control, CHC, Cav1 or SNX1 siRNA. The down-regulation of individual genes was analyzed by flow cytometry at 48 h-post transfection. The data are normalized to the expression of individual genes in Vero-E6 cells that were transfected with control siRNAs. The experiment was performed three times independently and the average values and their standard deviations are shown for each condition. **, $P < 0.01$ versus respective control (Student's *t* test). (b) The effect of knock down of target genes in Vero-E6 cells on EBV transmission mediated by cell-to-cell contact. Vero-E6 cells were transfected with control, CHC, Cav1 or SNX1 siRNAs. At 48 h post-transfection, the Vero-E6 cells were co-cultured with Akata$^-$ EBV-eGFP cells for 24 h. The percentages of eGFP-expressing Vero-E6 cells were analyzed by flow cytometry. The data are normalized to the expression of eGFP Vero-E6 cells that were transfected with a control siRNA. The experiment was performed three times independently and the average values and their standard deviations are shown for each condition. **, $P < 0.01$ versus respective control (Student's *t* test). (c) The knock down efficiency of CHC in Vero-E6 cells. Vero-E6 cells were transfected with a control or CHC siRNA. The knock down of the target gene was analyzed by flow cytometry at 48 h-post transfection. The data are normalized to expression of CHC in Vero-E6 cells that were transfected with a control siRNA. The

experiment was performed three times independently and the average values and their standard deviations are shown for each condition. **, $P < 0.01$ versus respective control (Student's *t* test). (d) The effect of cell contact on clathrin-mediated endocytosis in Vero-E6 cells. Vero-E6 cells were transfected with control or CHC siRNAs. At 48 h post-transfection, the Vero-E6 cells were co-cultured with Akata^{+} or Akata^{-} cells for 6 h at 37°C. The co-cultured cells were further incubated in the presence of 2 μg/ml AlexaFluor 594-transferrin for 10 min at 37°C. The Vero-E6 cells were harvested by trypsin and fixed with 4% PFA. The uptake of AlexaFluor 594-transferrin was analyzed by flow cytometry. The data are normalized to the uptake of 594-transferrin in Vero-E6 cells that were transfected with a control siRNA without co-cultivation. The experiment was performed three times independently and the average values and their standard deviations are shown for each condition. **, $P < 0.01$ versus respective control (Student's *t* test).

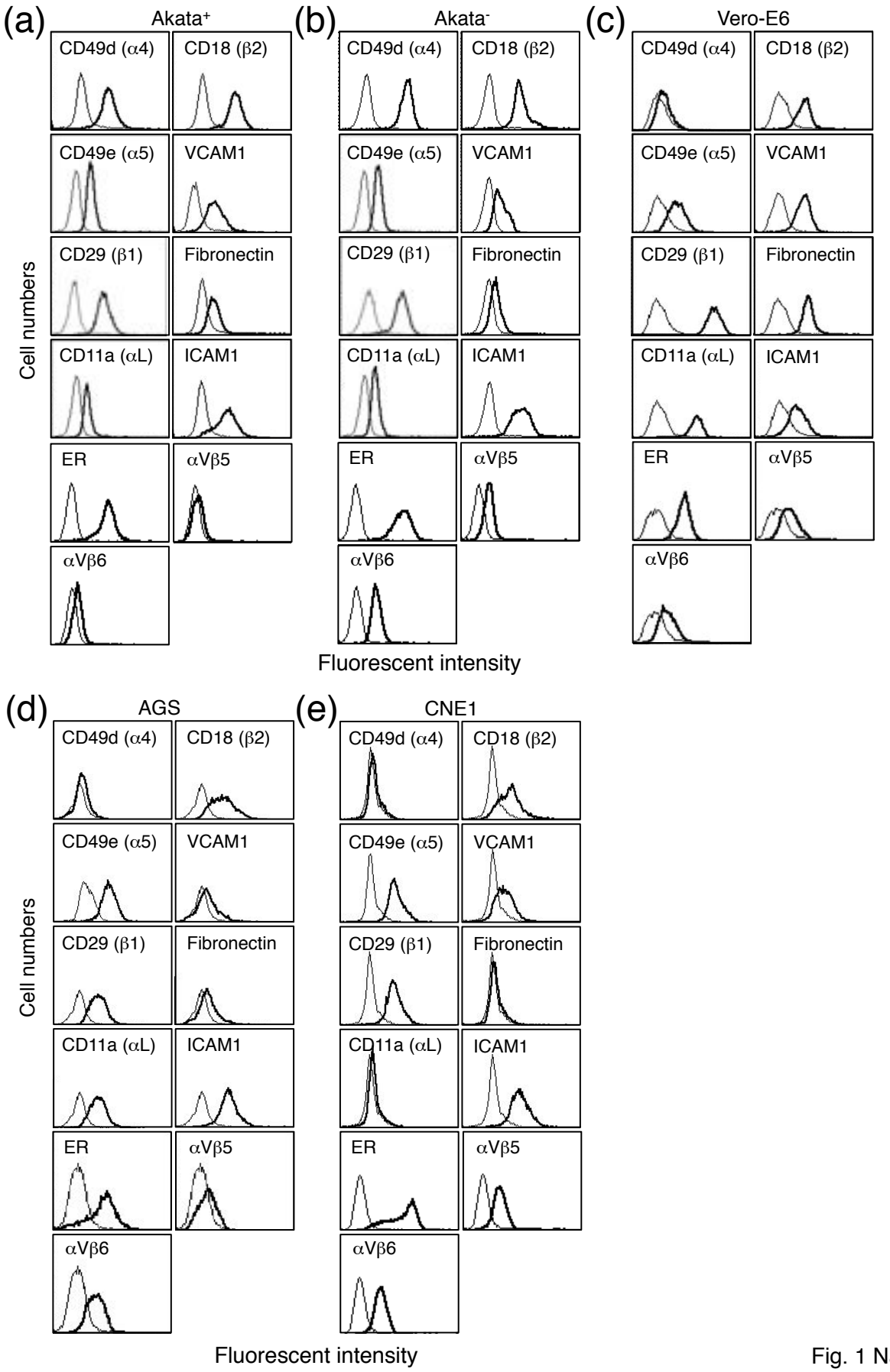

Fig. 1 Nanbo *et al.*

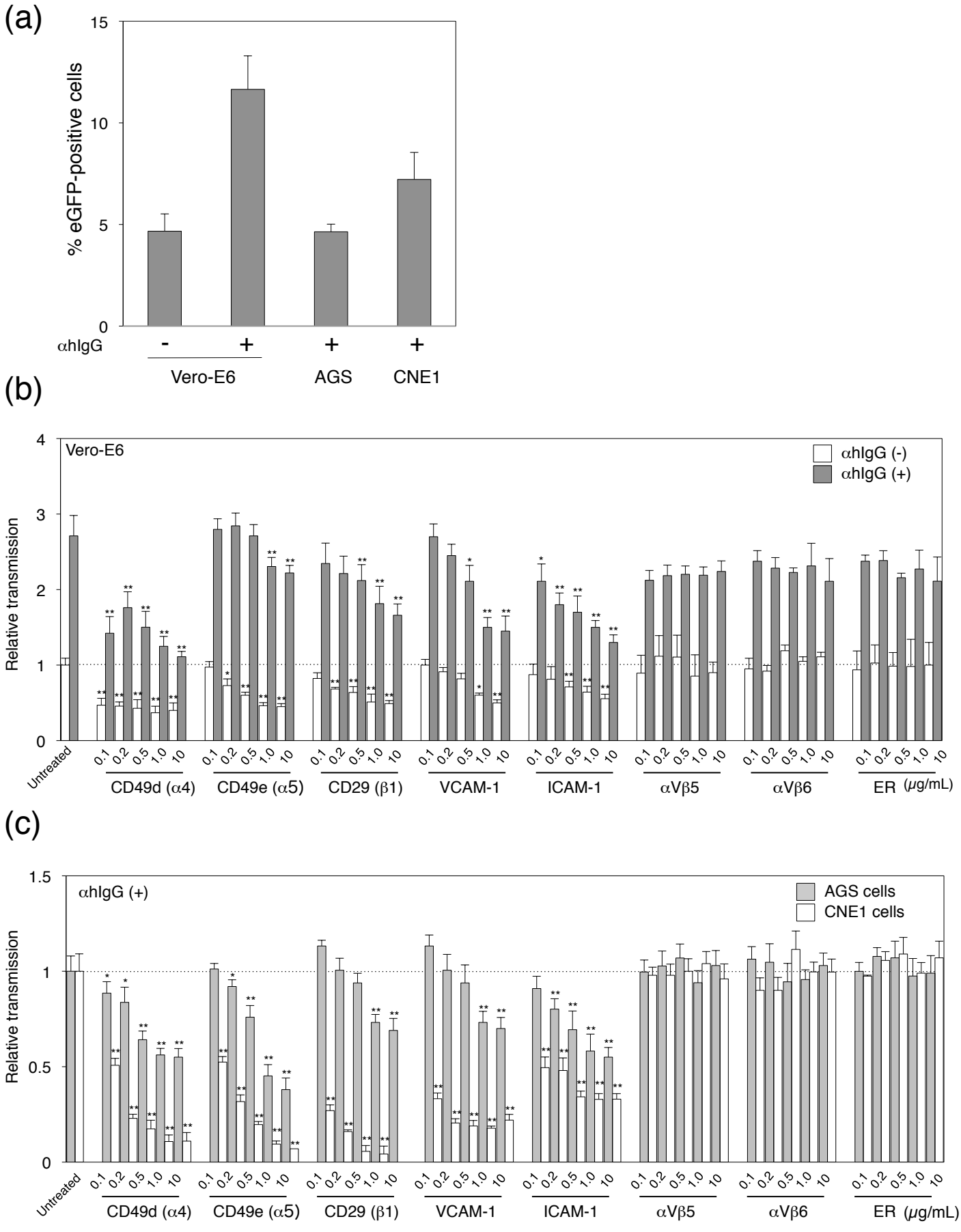

Fig. 2 Nanbo *et al.*

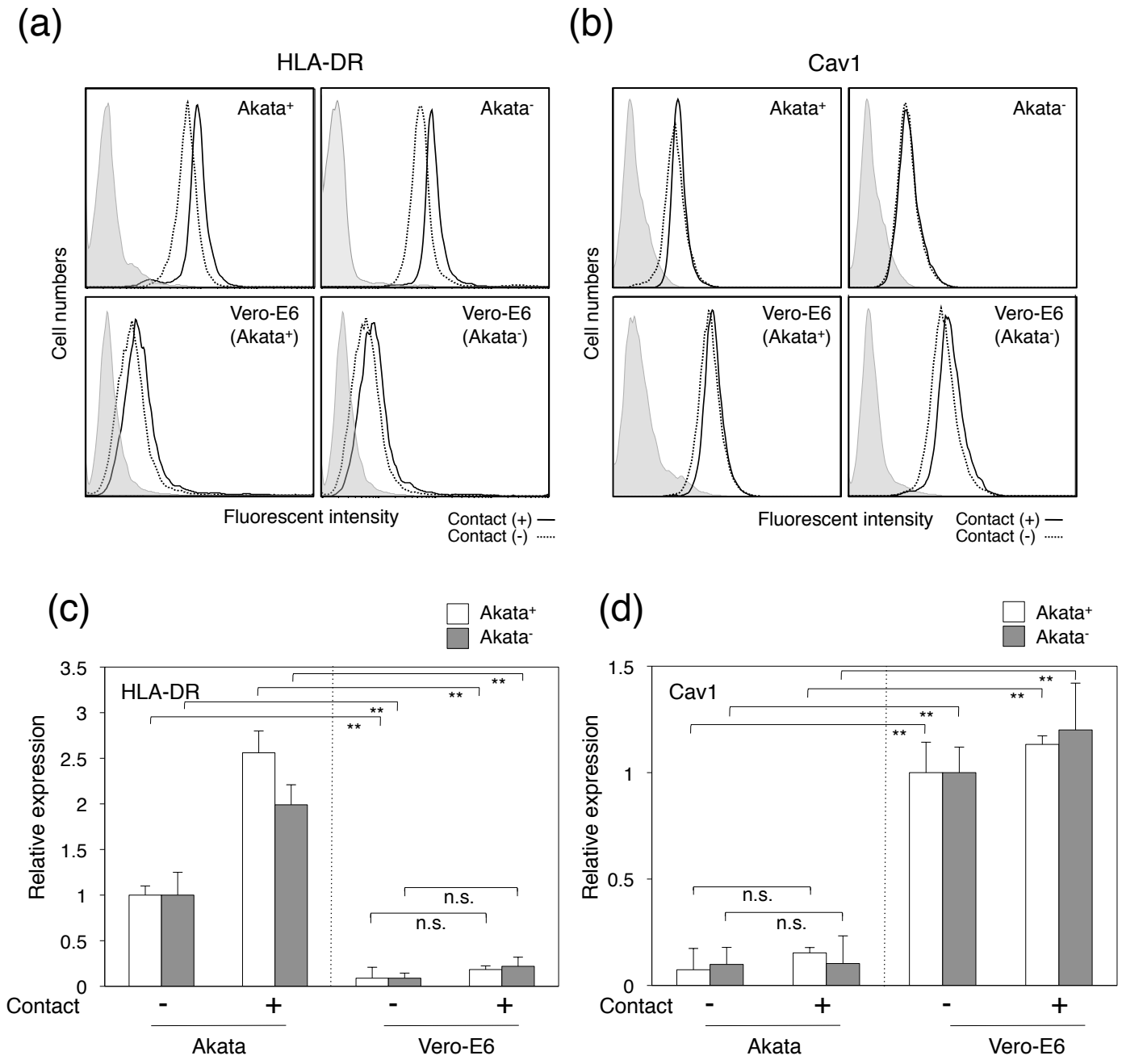

Fig. 3 Nanbo *et al. (continued)*

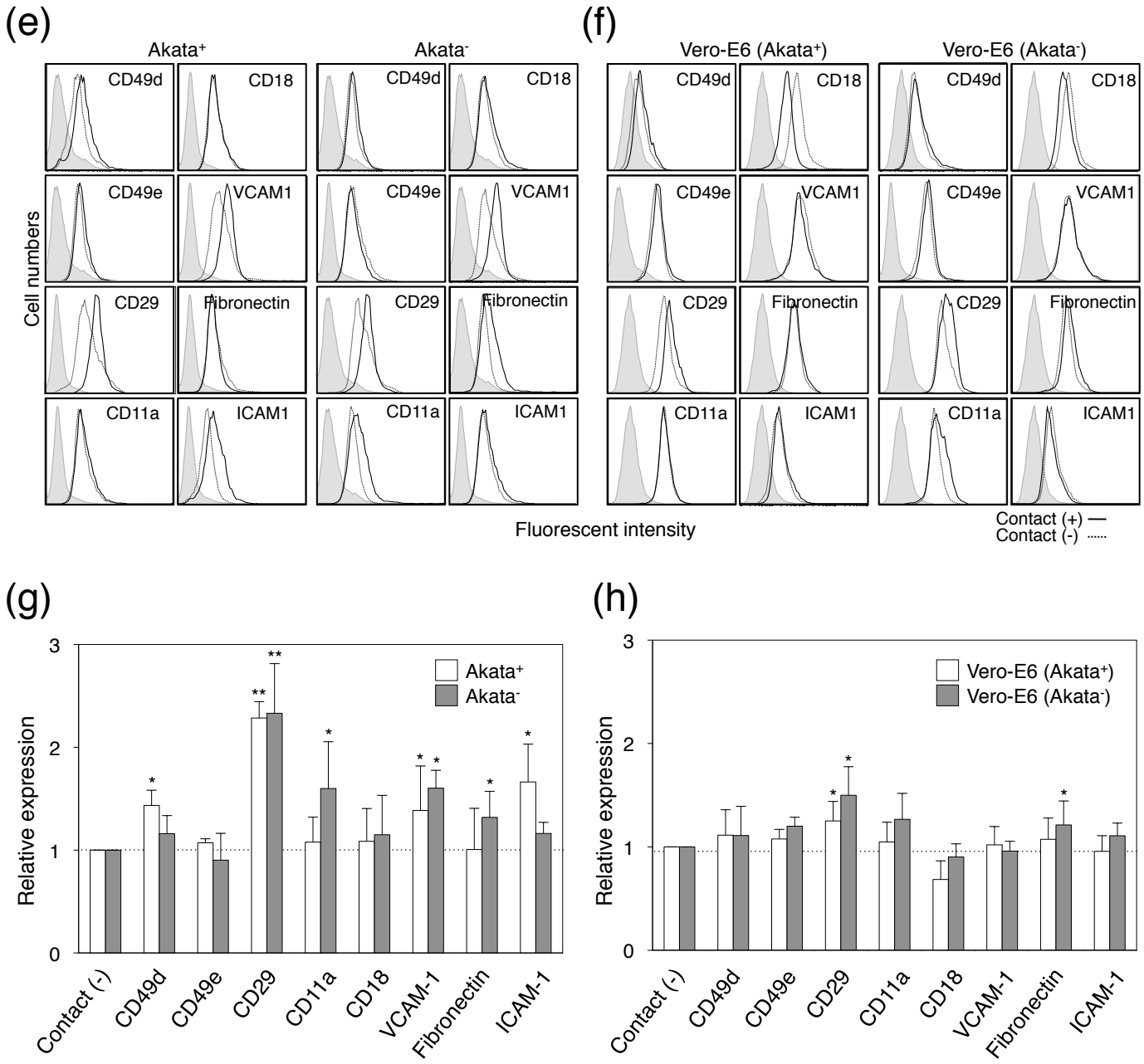

Fig. 3 Nanbo *et al.*

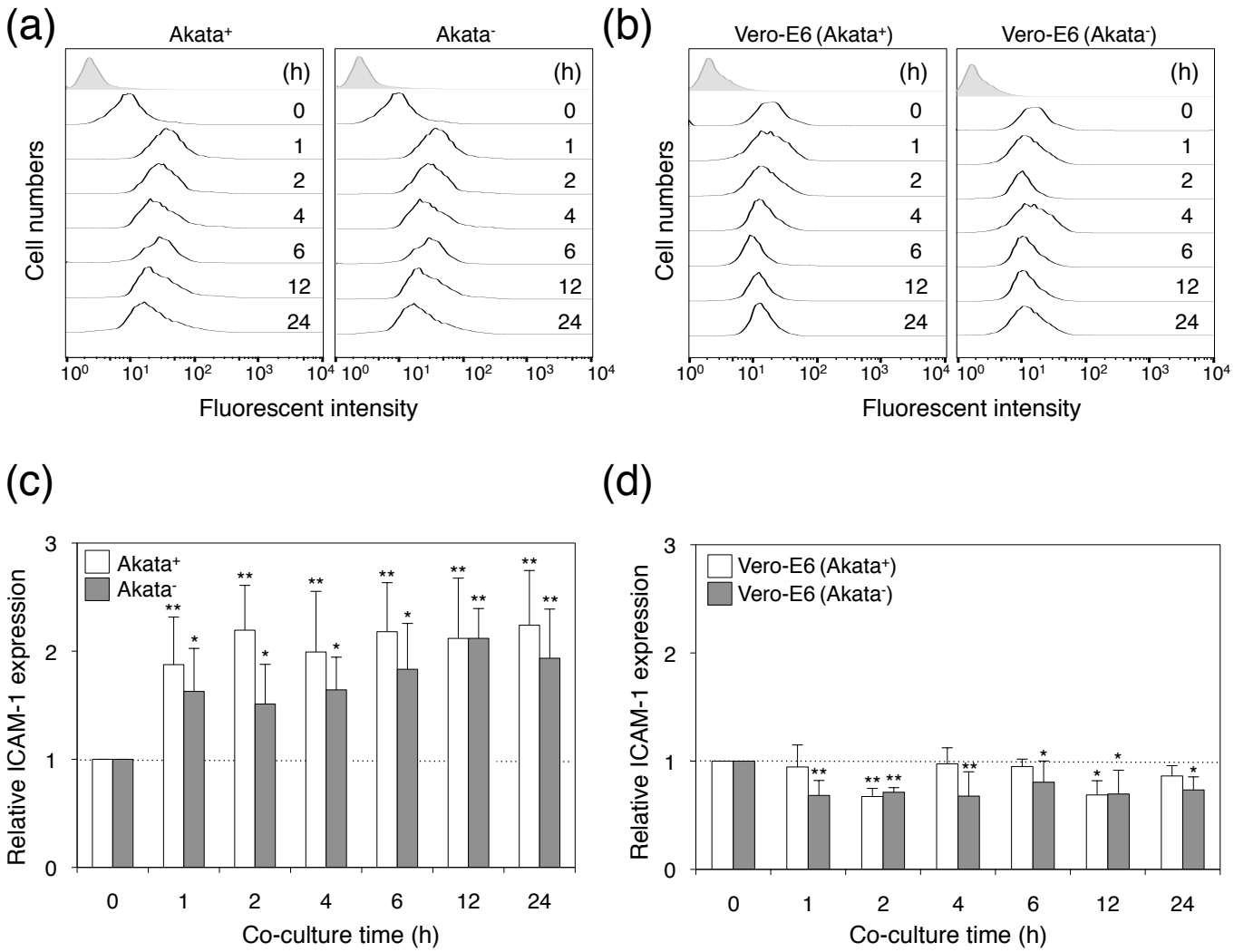

Fig. 4 Nanbo *et al. (continued)*

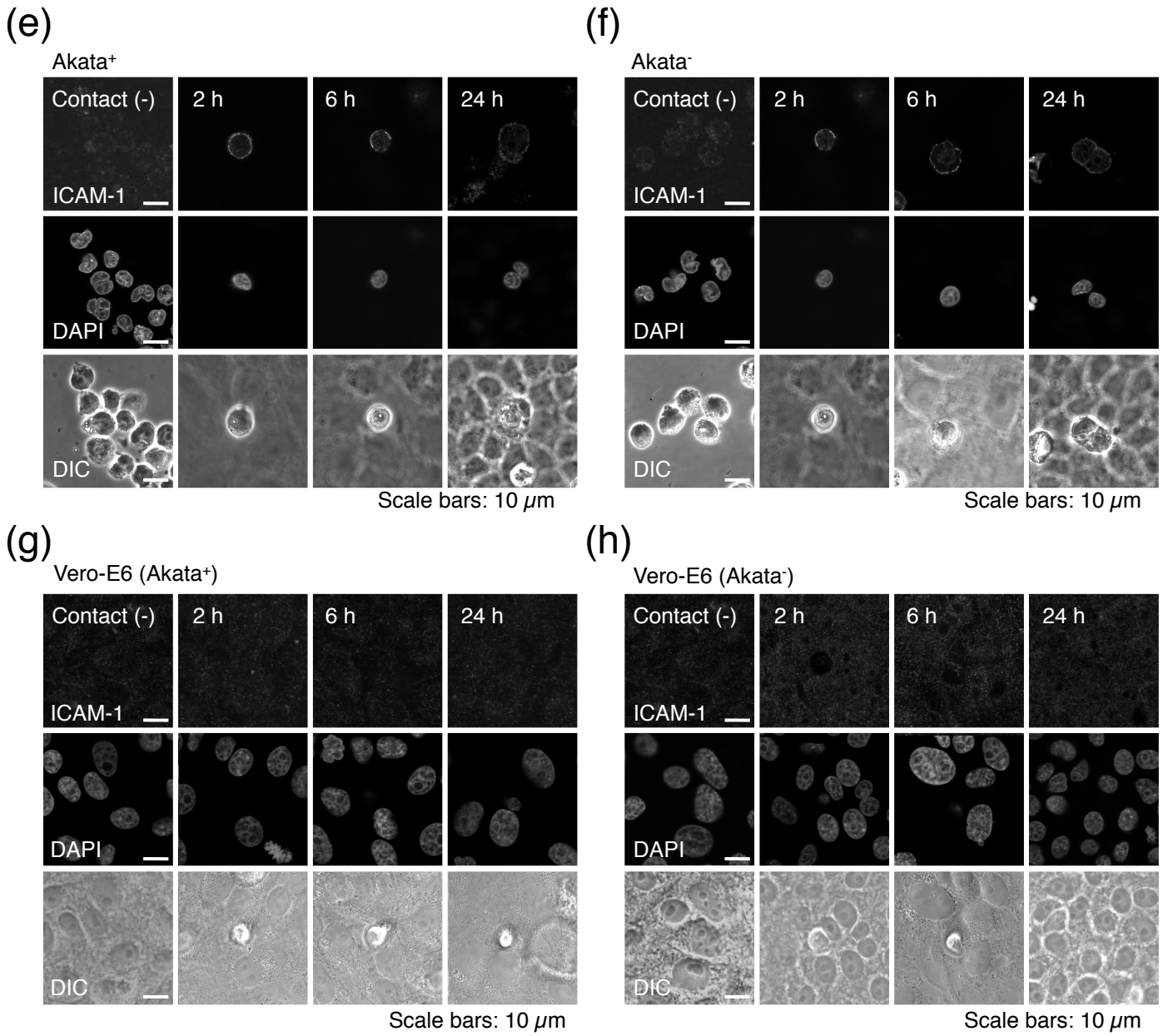

Fig. 4 Nanbo *et al.*

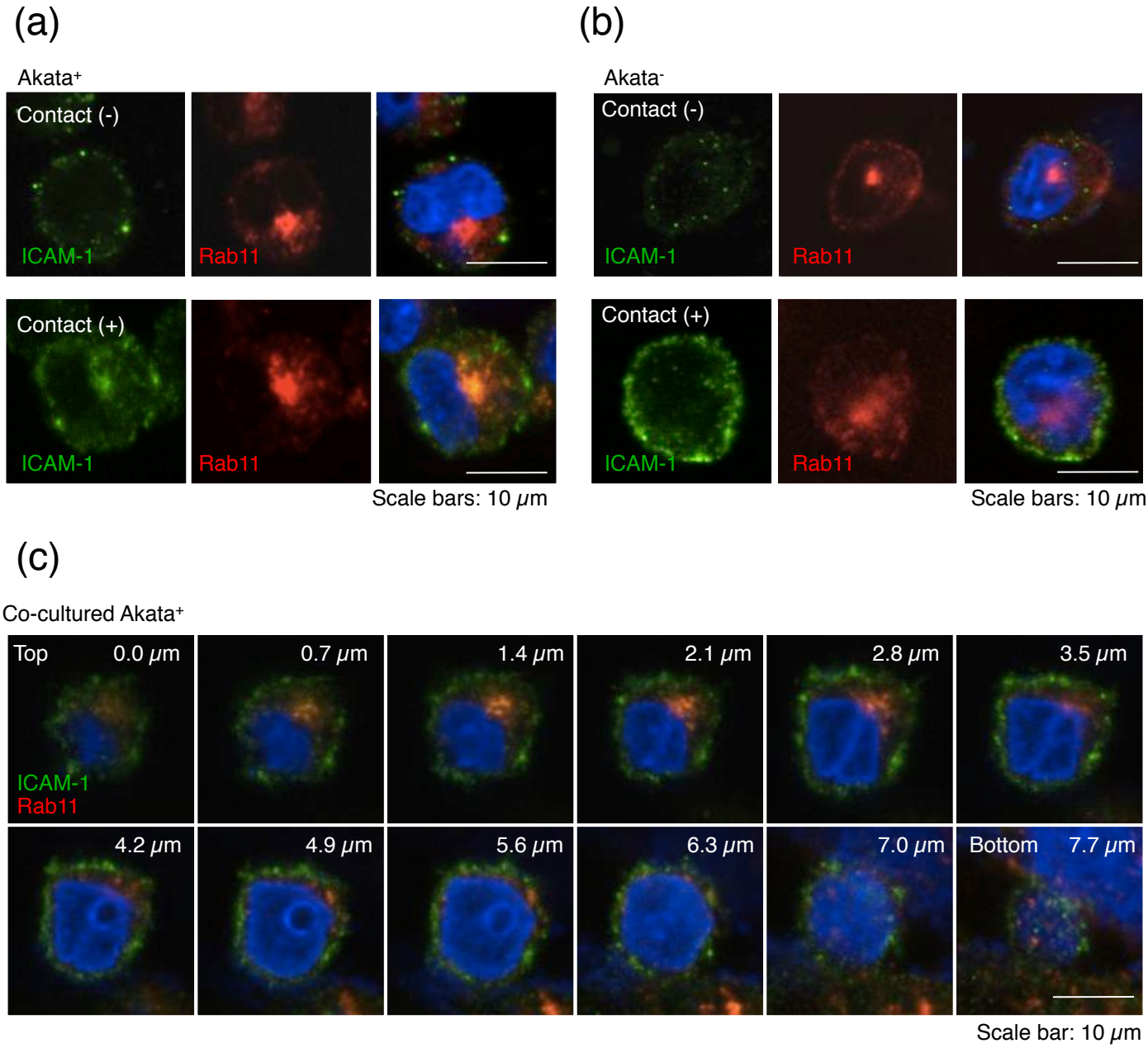

Fig. 5 Nanbo *et al.*

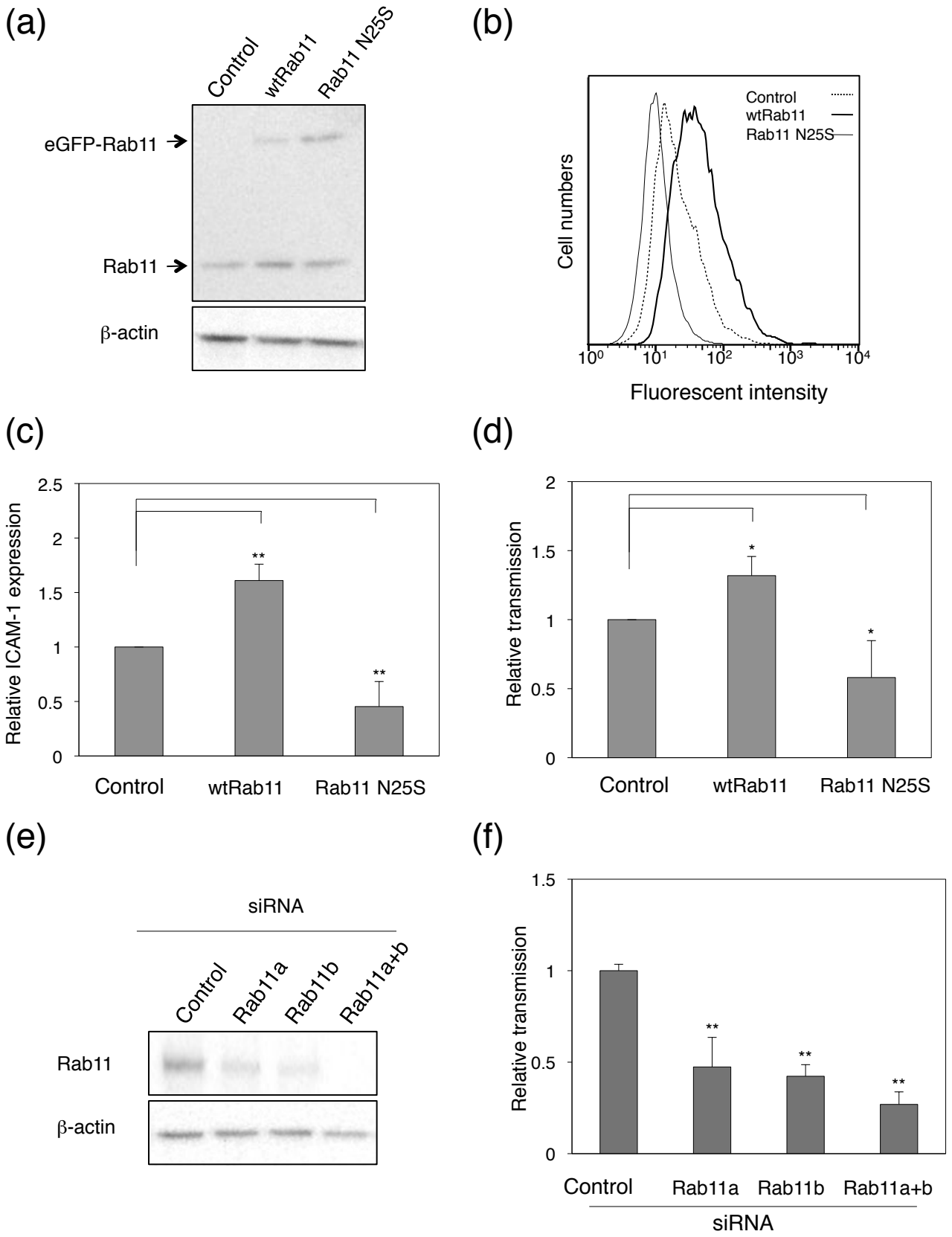

Fig. 6 Nanbo *et al.*

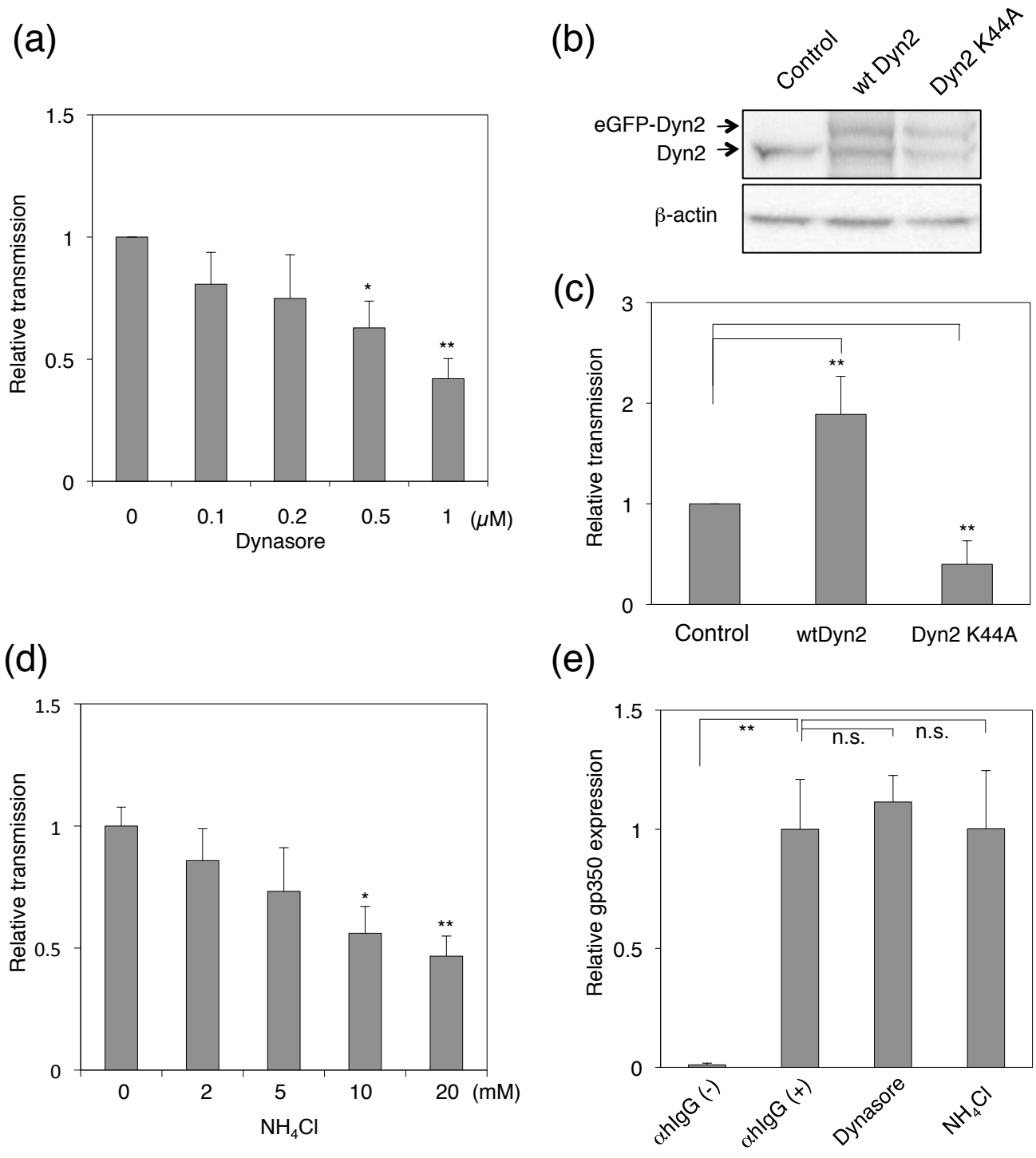

Fig. 7 Nanbo *et al.*

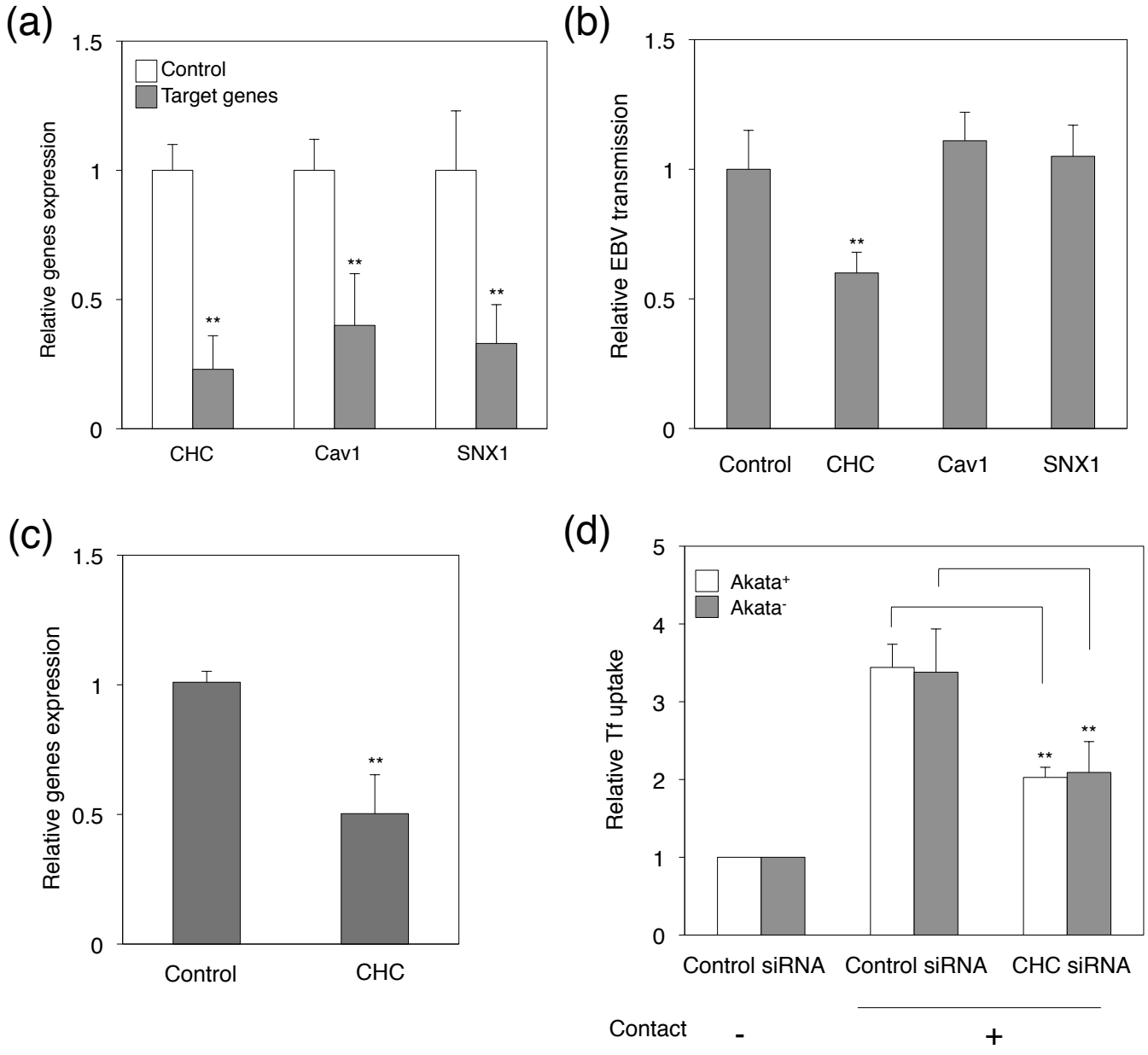

Fig. 8 Nanbo *et al.*